A Chiral Phosphoramidite beyond Monodentate Coordination: Secondary π-Interactions Turn a Dangling Aryl into a Two-, Four-, or Six-Electron Donor in d^6 and d^8 Complexes

Igor S. Mikhel, Heinz Rüegger, Pietro Butti, Francesco Camponovo, Dominik Huber, and Antonio Mezzetti*

Department of Chemistry and Applied Biosciences, ETH Zürich, CH-8093 Zürich, Switzerland

Received January 24, 2008

A study of the secondary interactions involving a pendant phenethyl group (NCH(CH_3)Ph) of (S_a,R_C,R_C)-O,O′-[1,1′-binaphthyl-2,2′-diyl]-*N*,*N*′-bis[1-phenylethyl]phosphoramidite (**1**) in d^8 and d^6 metal complexes is reported. A 1,2-η-phenyl interaction is found in [Pd(η^3-allyl)(1,2-η-Ph-**1**-κP)]$^+$ (**3**), as indicated by NMR spectroscopy and by an X-ray study. The Rh(I) complexes [RhCl(NBD)(**1**-κP)] (**4a**) and [RhCl(COD)(**1**-κP)] (**4b**) were prepared, and their X-ray structures were determined. Chloride abstraction from **4a** and **4b** gave the corresponding cations [Rh(NBD)(1,2-η-Ph-**1**-κP)]$^+$ (**5a**) and [Rh(COD)(1,2-η-Ph-**1**-κP)]$^+$ (**5b**), which were fully characterized. Besides NMR spectroscopic data, the 1,2-η-phenyl interaction is supported by an X-ray study of **5a**. Upon standing in MeOH solution, **5b** undergoes loss of the COD and forms [Rh(**1**-κP)(η^6-Ph-**1**-κP)]$^+$ (**6**), whose η^6-arene coordination was studied by NMR spectroscopy and by X-ray diffraction. For the sake of comparison with the d^8 complex **6**, the crystal structure of the previously reported d^6 analogue [$RuCl_2$(η^6-Ph-**1**-κP)]$^+$ (**7**) was determined. This study shows that secondary π-arene−metal interactions turn phosphoramidite **1** to a four-, six-, or eight-electron donor, with increasing bond strength in this order.

Introduction

Following early reports of the copper-catalyzed asymmetric conjugate addition of dialkylzinc to enones,[1] chiral phosphoramidites have attracted growing attention as novel chiral ligands in asymmetric catalysis. Moreover, chiral phosphoramidite ligands have become increasingly important because of their modularity, robustness, and low cost. In particular, binaphthol- or biphenol-based phosphoramidites containing aryl substituents at nitrogen have found application in hydrogenation,[2] hydrovinylation,[3] copper-catalyzed allylic substitution,[4] conjugate addition of boronic acids,[5] and the addition of organoaluminum reagents to carbonyl compounds.[6] In these applications, phosphoramidite ligands are generally considered to bind only with phosphorus and, thus, have attracted much interest in the wake of a renaissance of chiral monodentate ligands.[7] However, it has been recently shown that iridium complexes of methyl-amino-substituted P* ligands readily undergo cyclometalation upon treatment with a base. The resulting complexes feature P,C-bidentate coordination with a metal-bound methylene carbon atom and efficiently catalyze allylic substitution reactions for enantioselective C−C and C−N bond formation.[8]

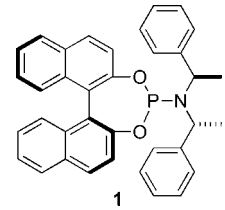

1

We have recently discovered yet a different P,C-bidentate mode, which involves the π-coordination of a dangling aryl substituent at nitrogen (phenyl (**1**) or 1-naphthyl) rather than C−H activation. Our original intention was to use a bulky phosphoramidite ligand to control the absolute configuration at the stereogenic metal atom of a half-sandwich cyclopropanation catalyst.[9] However, chloride abstraction from [$RuCl_2$(η^6-*p*-cymene)(P*-κP)] gave [RuCl(η^6-*p*-cymene)(1,2-η-Ph-P*-κP)]-PF_6 (**2**), in which one of the phenyl (or naphthyl) substituents at nitrogen of the phosphoramidite (P*) coordinates in an 1,2-

* Corresponding author. E-mail: mezzetti@inorg.chem.ethz.ch.

(1) (a) Feringa, B. L. *Acc. Chem. Res.* **2000**, *33*, 346. (b) Alexakis, A.; Trevitt, G. P.; Bernardinelli, G. *J. Am. Chem. Soc.* **2001**, *123*, 4358.

(2) (a) van den Berg, M.; Minnaard, A. J.; Haak, R. M.; Leeman, M.; Schudde, E. P.; Meetsma, A.; Feringa, B. L.; de Vries, A. H. M.; Maljaars, C. E. P.; Willans, C. E.; Hyett, D.; Boogers, J. A. F.; Henderickx, H. J. W.; de Vries, J. G. *Adv. Synth. Catal.* **2003**, *345*, 308. (b) Panella, L.; Aleixandre, A. M.; Kruidhof, G. J.; Robertus, J.; Feringa, B. L.; de Vries, J. G.; Minnaard, A. J. *J. Org. Chem.* **2006**, *71*, 2026.

(3) (a) Franciò, G.; Faraone, F.; Leitner, W. *J. Am. Chem. Soc.* **2002**, *124*, 736. (b) Kumareswaran, R.; Nandi, M.; RajanBabu, T. V. *Org. Lett.* **2003**, *5*, 4345. (c) Hölscher, M.; Franciò, G.; Leitner, W. *Organometallics* **2004**, *23*, 5606.

(4) (a) Malda, H.; van Zijl, A. W.; Arnold, L. A.; Minnaard, A. J.; Feringa, B. L. *Org. Lett.* **2001**, *3*, 1169. (b) Tissot-Croset, K.; Polet, D.; Alexakis, A. *Angew. Chem., Int. Ed. Engl.* **2004**, *43*, 2426.

(5) (a) Duursma, A.; Hoen, R.; Schuppan, J.; Hulst, R.; Minnaard, A. J.; Feringa, B. L. *Org. Lett.* **2003**, *5*, 3111. (b) Monti, C.; Gennari, C.; Piarulli, U. *Chem.−Eur. J.* **2007**, *13*, 1547.

(6) Biswa, K.; Chapron, A.; Cooper, T.; Fraser, P. K.; Novak, A.; Prieto, O.; Woodward, S. *Pure Appl. Chem.* **2006**, *78*, 511.

(7) (a) Lagasse, F.; Kagan, H. B. *Chem. Pharm. Bull.* **2000**, *48*, 315. (b) Komarov, I. V.; Börner, A. *Angew. Chem., Int. Ed.* **2001**, *40*, 1197.

(8) (a) Helmchen, G.; Dahnz, A.; Dubon, P.; Schelwies, M.; Weihofen, R. *Chem. Commun.* **2007**, 675. (b) Markovic, D.; Hartwig, J. F. *J. Am. Chem. Soc.* **2007**, *129*, 11680, and references therein. See also: (c) Polet, D.; Alexakis, A.; Tissot-Croset, K.; Corminboeuf, C.; Ditrich, K. *Chem.−Eur. J.* **2006**, *12*, 3596. (d) Lyothier, I.; Defieber, C.; Carreira, E. M. *Angew. Chem., Int. Ed.* **2006**, *45*, 6204.

(9) Huber, D.; Mezzetti, A. *Tetrahedron: Asymmetry* **2004**, *15*, 2193.

10.1021/om800064r CCC: $40.75
Publication on Web 06/18/2008

Scheme 1

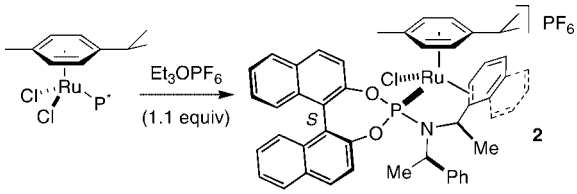

η-fashion to ruthenium (Scheme 1) instead of the expected 16-electron species.[10]

Although the η^2-coordination of a dangling benzyl group of ligand **1** has been proposed for nickel(0)[3c,6] and to explain[11] the enantioselectivity of palladium(II)[12] catalysts, well-characterized examples thereof have not been reported yet. This is surprising, as secondary metal−ligand interactions have been receiving increasing attention in catalysis, in particular in connection with palladium.[11] In this context, several Pd(II),[13–15] Pd(0),[16] and Pd(I)[17] catalysts for C−C bond formation containing bulky phosphine ligands have been found to feature secondary interactions to a dangling aryl group. In contrast to **2**, these palladium complexes generally feature a heteroatom substituent in the aryl group of the ligand, which might promote its coordination. In a distinct class of complexes that encompasses some BINAP ruthenium(II) complexes and related species,[18] the coordinated aryl is part of a chelate ring instead of a "dangling" substituent.

As part of our research in this area, we show herein that a π-aryl interaction of phosphoramidites bearing a pendant phenethyl group at the nitrogen atom is possible not only in d^6 complexes but also with d^8 metal ions, as in the new complex

Scheme 2

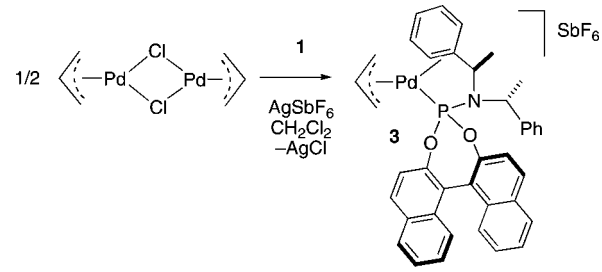

Chart 1

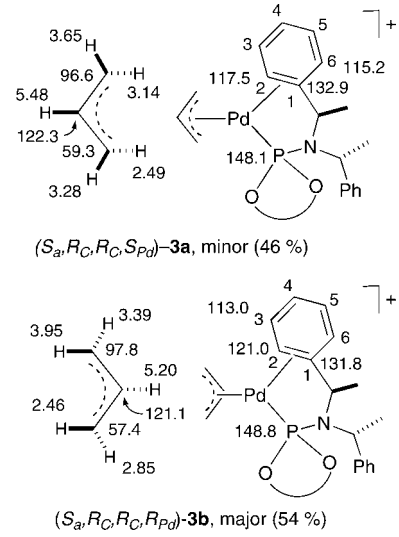

$[Pd(\eta^3\text{-allyl})(1,2\text{-}\eta\text{-Ph-}\mathbf{1}\text{-}\kappa P)]^+$ (**3**), in which the phenyl group of a NCH(Me)Ph binds in a 1,2-η-fashion to palladium. Additionally, we discuss the structural changes that occur upon aryl coordination in rhodium(I) complexes of the type [RhCl(diene)(**1**-κP)], $[Rh(diene)(1,2\text{-}\eta\text{-Ph-}\mathbf{1}\text{-}\kappa P)]^+$, and $[Rh(\mathbf{1}\text{-}\kappa P)(\eta^6\text{-Ph-}\mathbf{1}\text{-}\kappa P)]^+$, as well as the crystal structure of the previously reported $[RuCl_2(\eta^6\text{-Ph-}\mathbf{1}\text{-}\kappa P)]$ (**7**).[10a] This series of organometallic compounds shows that the aryl ring can act as a two-, four-, or six-electron donor according to the electronic requirements of the metal center.

Results and Discussion

$[Pd(\eta^3\text{-allyl})(1,2\text{-}\eta\text{-Ph-1-}\kappa P)]SbF_6$ (3). The reaction of $[PdCl(\eta^3\text{-allyl})]_2$ with ligand **1** (2 equiv) in CH_2Cl_2, followed by chloride abstraction with $AgSbF_6$, gave the corresponding cation $[Pd(\eta^3\text{-allyl})(1,2\text{-}\eta\text{-Ph-}\mathbf{1}\text{-}\kappa P)]^+$ (**3**) (Scheme 2), which was isolated and fully characterized as the SbF_6^- salt. The ^{31}P NMR spectrum in CD_2Cl_2 shows two singlets at δ 148.1 (minor isomer **3a**) and at 148.8 (major isomer **3b**), whose integration indicates that $[Pd(\eta^3\text{-allyl})(1,2\text{-}\eta\text{-Ph-}\mathbf{1}\text{-}\kappa P)]^+$ exists as a 46:54 mixture of diastereoisomers. A combination of X-ray and NMR spectroscopic studies indicate that the absolute configuration at palladium is S_a,R_C,R_C,S_{Pd} for the minor diastereoisomer **3a** and S_a,R_C,R_C,R_{Pd} for the major one **3b** (Chart 1).[19] In contrast with the ^{31}P NMR spectrum, which is essentially invariant between room temperature and −90 °C, the ^1H NMR spectrum is temperature dependent and indicates a highly dynamic behavior.

(10) (a) Huber, D.; Kumar, P. G. A.; Pregosin, P. S.; Mikhel, I. S.; Mezzetti, A. *Helv. Chim. Acta* **2006**, *89*, 1696. (b) Huber, D.; Kumar, P. G. A.; Pregosin, P. S.; Mezzetti, A. *Organometallics* **2005**, *24*, 5221.

(11) For a review on secondary interactions in asymmetric hydrosilylation, see:(a) Gibson, S. E.; Rudd, M. *Adv. Synth. Catal.* **2007**, *349*, 781.

(12) Jensen, J. F.; Svendsen, B. Y.; La Cour, T. V.; Pedersen, H. L.; Johannsen, M. *J. Am. Chem. Soc.* **2002**, *124*, 4558.

(13) Selected papers on MAP, MOP, and related ligands:(a) Lloyd-Jones, G. C.; Stephen, S. C.; Murray, M.; Butts, C. P.; Vyskocyl, S.; Kocovsky, P. *Chem.−Eur. J.* **2000**, *6*, 4348. (b) Wang, Y.; Li, X.; Sun, J.; Ding, K. *Organometallics* **2003**, *22*, 1856. (c) Kumar, P. G. A.; Dotta, P.; Hermatschweiler, R.; Pregosin, P. S.; Albinati, A.; Rizzato, S. *Organometallics* **2005**, *24*, 1306. (d) Faller, J. W.; Sarantopoulos, N. *Organometallics* **2004**, *23*, 2008.

(14) Bidentate σ,1,2-η-arylalkyl ligands (selected papers):(a) Ossor, H.; Pfeffer, M.; Jastrzebski, J. T. B. H.; Stam, C. H. *Inorg. Chem.* **1987**, *26*, 1169. (b) Li, C.-S.; Cheng, C.-H.; Liao, F.-L.; Wang, S.-L. *J. Chem. Soc., Chem. Commun.* **1991**, 710. (c) Li, C.-S.; Jou, D.-C.; Cheng, C.-H. *Organometallics* **1993**, *12*, 3945. (d) Reddi, K. R.; Surekha, K.; Lee, G.-H.; Peng, S.-M.; Liu, S.-T. *Organometallics* **2001**, *20*, 5557. (e) Catellani, M.; Mealli, C.; Motti, E.; Paoli, P.; Perez-Carreno, E.; Pregosin, P. S. *J. Am. Chem. Soc.* **2002**, *124*, 4336.

(15) Pd(II) BINOL complexes:(a) Bergens, S. H.; Leung, P. H.; Bosnich, B.; Rheingold, A. L. *Organometallics* **1990**, *9*, 2406. (b) Brunkan, N. M.; Gagne, M. R. *Organometallics* **2002**, *21*, 4711.

(16) (a) Barder, T. E.; Walker, S. D.; Martinelli, J. R.; Buchwald, S. L. *J. Am. Chem. Soc.* **2005**, *127*, 4685. (b) Marshall, W. J.; Grushin, V. V. *Organometallics* **2003**, *22*, 555. (c) Reid, S. M.; Boyle, R. C.; Mague, J. T.; Fink, M. J. *J. Am. Chem. Soc.* **2003**, *125*, 7816. (d) Yin, J.; Rainka, M. P.; Zhang, X.-X.; Buchwald, S. L. *J. Am. Chem. Soc.* **2002**, *124*, 1162.

(17) Recent papers:(a) Barder, T. E. *J. Am. Chem. Soc.* **2006**, *128*, 898. (b) Christmann, U.; Pantazis, D. A.; Benet-Buchholz, J.; McGrady, J. E.; Maseras, F.; Vilar, R. *J. Am. Chem. Soc.* **2006**, *128*, 6376. (c) Dotta, P.; Kumar, P. G. A.; Pregosin, P. S.; Albinati, A.; Rizzato, S. *Organometallics* **2004**, *23*, 4247.

(18) (a) Pathak, D. D.; Adams, H.; Bailey, N. A.; King, P. J.; White, C. *J. Organomet. Chem.* **1994**, *237*, 237. (b) Feiken, N.; Pregosin, P. S.; Trabesinger, G.; Albinati, A.; Evoli, G. L. *Organometallics* **1997**, *16*, 5756. (c) Cyr, P. W.; Rettig, S.; Patrick, B. O.; James, B. R. *Organometallics* **2002**, *21*, 4672. (d) Doherty, S.; Knight, J. G.; Rath, R. K.; Clegg, W.; Harrington, R. W.; Newman, C. R.; Campbell, R.; Amin, H. *Organometallics* **2005**, *24*, 2633.

(19) We use here the convention suggested by Faller and Sarantopoulos,[13d] which regards the allyl as an 18-electron pseudoatom placed at the centroid of the allyl. Stereodescriptors assume that the priorities are allyl > P > 1,2-η-phenyl and the centroid of the allyl is out of the plane in the direction of the central carbon atom.

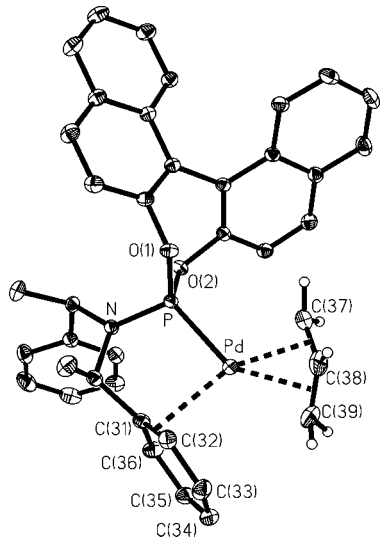

Figure 1. ORTEP drawing of the $[Pd(\eta^3\text{-}C_3H_5)(1,2\text{-}\eta\text{-Ph-}\mathbf{1}\text{-}\kappa P)]^+$ cation, (S_a,R_C,R_C,S_{Pd})-**3a**.

Table 1. Selected Bond Lengths (Å) and Angles (deg) for (S_a,R_C,R_C,S_{Pd})-3a

Pd−P	2.2598(5)	Pd−C(37)	2.111(2)
Pd−C(38)	2.163(3)	Pd−C(39)	2.250(3)
Pd−C(31)	2.513(2)	Pd−C(32)	2.413(2)
Pd···C(33)	3.065(2)	Pd···C(36)	3.147(2)
C(31)−C(32)	1.408(3)	C(32)−C(33)	1.407(3)
C(33)−C(34)	1.382(4)	C(34)−C(35)	1.378(4)
C(35)−C(36)	1.376(3)	C(31)−C(36)	1.408(3)
C(37)−C(38)	1.362(5)	C(38)−C(39)	1.298(5)
P−Pd−C(37)	97.34(8)	P−Pd−C(39)	162.89(9)
P−Pd−C(32)	102.79(6)	P−Pd−C(31)	78.06(5)
C(37)−Pd−C(39)	66.14(11)	C(32)−Pd−C(39)	94.30(10)
C(37)−Pd−C(31)	168.53(9)	C(37)−Pd−C(32)	156.82(9)

At −90 °C, reasonably resolved spectra are obtained, which indicate the same isomer distribution as at room temperature.

The absolute configuration at palladium was assigned on the basis of distance constraints from nuclear Overhauser effects involving the methyl group of the coordinated N-CH(CH_3)Ph moiety and the five protons of the allyl group. For the minor isomer **3a**, the strongest interaction is observed to the central allyl proton, followed by those to the two *syn*-protons. This is consistent with the same allyl orientation as found by the X-ray analysis, that is, S_{Pd}-configuration at the metal. For the major isomer **3b**, the strongest interaction is found for the *anti*-proton *trans* to the phosphorus donor, the second *anti*-proton following, whereas no interaction is found for the central allyl proton. This is consistent with the opposite orientation of the allyl, that is, with R_{Pd} stereochemistry at the metal center.

Crystals of $[Pd(\eta^3\text{-allyl})(1,2\text{-}\eta\text{-Ph-}\mathbf{1}\text{-}\kappa P)]SbF_6$ (**3**) were grown by slow diffusion of hexane into dichloromethane. The coordination geometry of palladium can be considered as slightly distorted square planar (Figure 1). As the absolute configuration of palladium is *S*, the crystal contains the S_a,R_C,R_C,S_{Pd} diastereoisomer **3a**. The Pd−C distances involving the terminal allyl C atoms reveal a strongly asymmetric coordination, the Pd−C distance *trans* to P being 0.14 Å longer than that *trans* to the 1,2-η-phenyl. The asymmetry (Δ(Pd−C)) of allyl coordination in **3a** is at the upper end of the range observed in the allyl derivatives containing MOP ((Δ(Pd−C) = 0.13 Å)[13a] and MAP (Δ(Pd−C = 0.11 Å)[13b] and is much larger than in a related complex, $[PdCl(\eta^3\text{-allyl})(P^*)]$ (Δ(Pd−C) = 0.03 Å), which

Chart 2

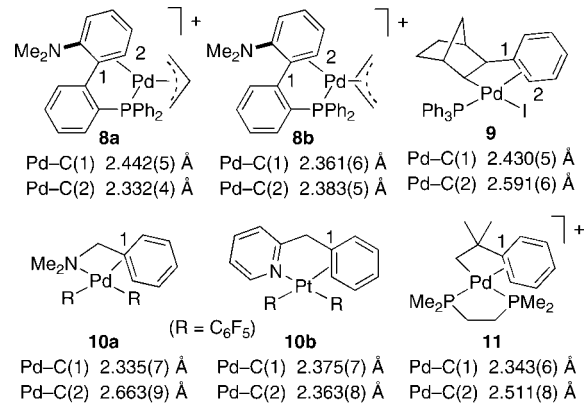

contains a monodentate phosphoramidite (P*).[20] As phosphoramidites[20] have been shown to exert a stronger *trans* influence than phosphines[21] in palladium(II) allyl complexes, the strong asymmetry of allyl coordination in **3** most probably derives from the combination of the weak Pd−(1,2-η-phenyl) interaction with the strong Pd−P bond.

The Pd−P distance (2.2598(5) Å) is slightly shorter than in the monodentate phosphoramidite complex $[PdCl(\eta^3\text{-allyl})(P^*)]$ mentioned above (2.2960(5) Å),[20] which can be explained with the chelate effect. The 1,2-η-coordinated phenyl ring is loosely bound, as indicated by the Pd−C_{ipso} and Pd−C_{ortho} separations of 2.513(2) and 2.413(2) Å, respectively, which suggest a weak, asymmetric η^2-interaction (Table 1). Not surprisingly, the η^2-arene−palladium distances are much longer in **3a** than in $[Pd(BINAPO,\kappa P)(1,2\text{-}\eta\text{-Np-BINAPO},\kappa P)]$ (2.160(3) and 2.228(3) Å),[16b] as the π-donation to the arene (in the latter case a naphthyl group) is stronger in the Pd(0) complex. Interestingly, also the Pd(II) complex $[Pd(\eta^3\text{-allyl})(1,2\text{-}\eta\text{-Np-MOP})]^+$ (2.338(6) and 2.474(6) Å) features a stronger η^2-coordination than **3a**.[13a] The same is true for $[Pd(\eta^3\text{-allyl})(1,2\text{-}\eta\text{-Ph-L})]^+$ (L = 2-(dicyclohexylphosphino)-2′-(dimethylamino)biphenyl), which exists as the isomers **8a** and **8b** (Chart 2).[13d] However, the stronger coordination of MOP, and of MAP in particular, might reflect the effect of the heteroatom substituent in the arene ring.[13a]

Besides metal−arene distances, the distortion from planarity of the ring is thought to be diagnostic of the strength of the arene−metal bond.[22,23] In **3a**, the phenyl ring is only very slightly distorted, the largest deviations from planarity being 0.023(2) Å away from Pd for C(31) and 0.018(2) Å toward Pd for C(32). Although the degree of pyramidalization of C(31) is very low (the sum of the C−C−C angles around it is 359.1°), the coordination to palladium does influence the 1,2-η-phenyl ring. Interestingly, the C−C distances fall into two clearly defined groups with mean values of 1.4077(6) Å in the C(36)−C(31)−C(32)−C(33) fragment and of 1.379(3) in the other half. The expansion of one-half of the phenyl ring is rare but has been observed in the related complex **8a**.[13d] This distortion is inconsistent with the expected π-bond localization[22,23] that results in the alternation of three long and three short C−C

(20) Boele, M. D. K.; Kamer, P. C. J.; Lutz, M.; Spek, A. L.; de Vries, J. G.; van Leeuwen, P. W. N. M.; van Strijdonck, G. P. F. *Chem.−Eur. J.* **2004**, *10*, 6232.

(21) See, for instance:(a) Albert, J.; Bosque, R.; Cadena, J. M.; Delgado, S.; Granell, J.; Muller, G.; Ordinas, J. I.; Bardia, M. F.; Solans, X. *Chem.−Eur. J.* **2002**, *8*, 2279.

(22) Muetterties, E. L.; Bleeke, J. R.; Wucherer, E. J.; Albright, T. A. *Chem. Rev.* **1982**, *82*, 199.

(23) Hubig, S. M.; Lindeman, S. V.; Kochi, J. K. *Coord. Chem. Rev.* **2000**, *200−202*, 831.

Scheme 3

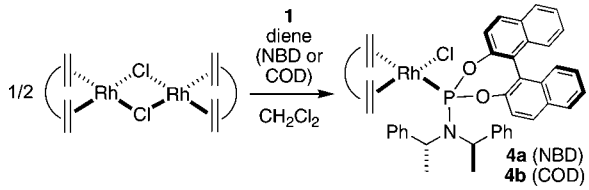

bonds, as observed in the η^2-coordination of phenyl to platinum(II).[24] We have no explanation for this observation at the moment.

The structural features of **3** are in agreement with the suggestion[23] that complexes of weak Lewis acidity, such as in the palladium complex **9** in Chart 2,[14b] preferentially give η^2-coordination. When electron-withdrawing groups increase the Lewis acidity of the metal center, such as R in **10a**,[25] the η^1-mode is thought to be favored. Accordingly, η^2-coordination is observed in the softer Pt(II) analogue **10b**.[24] The transition between the η^1- and η^2-coordination modes is smooth and continuous, though. Thus, the phenyl coordination in **11** has been described as π-η^1 (Chart 2), but the Pd−phenyl distances are similar to those of **3a**.[26] Besides electronic effects, steric hindrance influences the coordination mode of the aryl. Perusal of Chart 2 suggests that chelate ring strain might favor the η^2-coordination in the five-membered chelates as compared to the (more strained) four-membered ones.[27]

NMR Spectroscopic Studies of 3. The key ^{13}C NMR signals of the Pd-bound phenyl of both isomers were located by a combination of NMR spectroscopic methods ($^{31}P-^{1}H$ HMQC, $^{13}C-^{1}H$ HMQC, $^{13}C-^{1}H$ HMBC, $^{1}H-^{1}H$ COSY, and $^{1}H-^{1}H$ NOESY) at −90 °C (Chart 1). Severe overlap in the ^1H NMR spectrum precluded the full assignment of the aromatic signals. The ^{13}C signals of the *ipso* carbons C^1 of the major and minor isomers appear at 132.9 (**3a**) and 131.8 (**3b**) and are shifted to lower frequency by ca. 7 ppm as compared to the uncoordinated phenyl rings at ca. δ 139 in the rhodium analogues **5a** and **5b** (see Table 5). The ^{13}C signals of the *ortho* C atoms are significantly shifted from the average value of uncoordinated phenyl ring to ca. δ 128. Surprisingly, the resonance of one *meta* C atom (C^3) in the major isomer **3b** is even more perturbed (113.0 vs ca. 129, average value for the *meta* C atoms). The same applies for C^6 in the minor isomer **3a** (δ 115.2 vs 128).

As the above data might be interpreted as suggestive of η^3-coordination of the aryl ring in solution, and in an effort to correlate in a reliable fashion the NMR spectroscopic data in solution with the crystal structure of **3a**, we recorded the solid-state CP-MAS ^{13}C NMR spectrum of **3**. Interestingly, this spectrum exhibits a broad, intense peak at δ 99.1 that is not observed in the solution spectra at −90 °C and results from the overlap of one allyl signal with an arene resonance. Unfortunately, this signal cannot be attributed unambiguously in view of its line-width, and we tentatively assign it to the *ortho* C atom C(32), which shows the shortest contact to palladium in the X-ray structure of **3a**. A coordination chemical shift $\Delta\delta$ of (at least) −28 can be assumed by comparison with the data of **5a** and **5b** (see Table 5). This is similar to the upfield

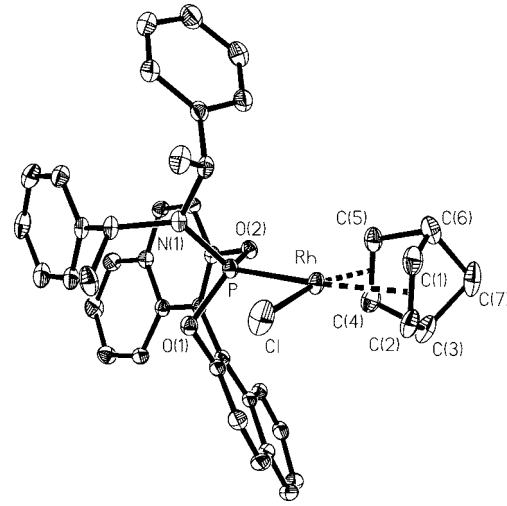

Figure 2. ORTEP drawing of [RhCl(NBD)(**1**,κP)], (S_a,R_c,R_c)-**4a**.

Table 2. Selected Bond Lengths (Å) and Angles (deg) for (S_a,R_C,R_C)-4a

Rh−P	2.2183(7)	Rh−Cl	2.3429(8)
Rh−C(1)	2.261(3)	Rh−C(2)	2.240(3)
Rh−C(4)	2.080(3)	Rh−C(5)	2.100(3)
P−Rh−C(1)	158.19(9)	P−Rh−C(2)	160.96(9)
P−Rh−C(4)	98.90(8)	P−Rh−C(5)	98.26(8)
Cl−Rh−C(1)	100.65(9)	Cl−Rh−C(2)	95.70(9)
Cl−Rh−C(4)	150.98(9)	Cl−Rh−C(5)	163.80(8)
Cl−Rh−P	92.06(3)		

coordination shifts ($\Delta\delta$) that have been observed previously for Pd(II) allyl complexes featuring 1,2-η-bound biaryls.[13a,d] Interestingly, the solid-state ^{13}C NMR spectrum contains no signals at δ 115 (C^6 signal in **3a**) and at δ 113 (C^3 signal in **3b**), which indicates that **3** might have (slightly) different structures in solution and in the solid state.

Summarizing, a correlation between ^{13}C NMR shifts and metal−arene distances is not straightforward owing to the high fluxionality of **3**. An additional problem is the apparent low sensitivity of the coordination chemical shifts to the metal−carbon distances. This is shown by the related diastereoisomeric complexes **8a** and **8b**, which feature similar $\Delta\delta$ values for the C_{ipso} and C_{ortho} atoms (−26.6 and −22.6 ppm, respectively), although the degree of asymmetry of the η^2-coordination in these diastereoisomers is very different (Chart 2).[13d] Details of the dynamic behavior of complexes of type **3** in solution, as well as DFT calculations concerning **3**, have been reported independently.[28]

Neutral Rh(I) Complexes. Ligand **1** readily reacts with [RhCl(diene)]$_2$ in CH_2Cl_2 at room temperature to give [RhCl(diene)(**1**-κP)] (diene = norbornadiene (**4a**), 1,5-cyclooctadiene (**4b**)) in nearly quantitative yields (Scheme 3). The ^{31}P NMR spectra in $CDCl_3$ show a doublet at δ 136.7 ($^1J_{Rh,P}$ = 280 Hz) and at δ 133.6 ($^1J_{Rh,P}$ = 247 Hz) for **4a** and **4b**, respectively. The COD derivative **4b** features a smaller $^1J_{Rh,P}$ coupling constant than

(24) Casas, J. M.; Fornies, J.; Martin, A.; Menjon, B. *Organometallics* **1993**, *12*, 4376.

(25) Falvello, L. R.; Fornies, J.; Navarro, R.; Sicilia, V.; Tomas, M. *J. Chem. Soc., Dalton Trans.* **1994**, 3143.

(26) Campora, J.; Gutierrez-Puebla, E.; Lopez, J. A.; Monge, A.; Palma, P.; del Rio, D.; Carmona, E. *Angew. Chem., Int. Ed.* **2001**, *40*, 3641.

(27) Also steric hindrance caused by 2,6-disubstitution, such as in [Pd(dba)(L)] (dba = dibenzylideneacetone, L = 2-(2′,6′-dimethoxybiphenyl)dicyclohexylphosphine), might favor η^1-coordination.[16a]

(28) Filippuzzi, S.; Pregosin, P. S.; Calhorda, M. J.; Costa, P. J. *Organometallics* **2008**, *27*, 2949, next paper in this issue. Details of DFT calculations: Amsterdam Density Functional (ADF2006) program, gradient-corrected geometry optimizations without symmetry constraints, local density approximation of the correlation energy (Vosko, Wilk, Nusair), exchange−correlation functionals of Perdew and Wang (PW91), ZORA approximation for relativistic effects, triple-ζ Slater-type orbital (STO) basis set augmented by two polarization functions (Pd, Ru, P, O, C, N, and H atoms), frozen core approximation for the core electrons: (1s) for C, O, and N, (1s, 2p) for P, ([1−3]s, [2−3]p, 3d) for Pd and Ru.

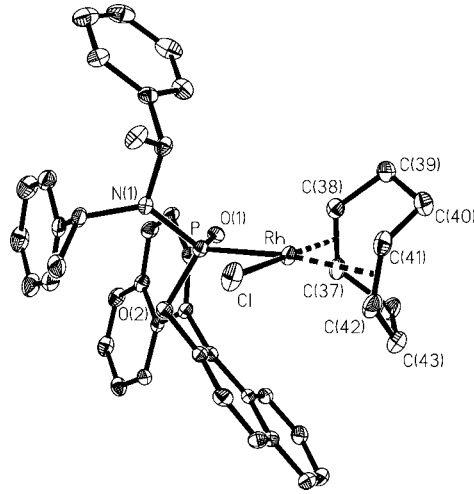

Figure 3. ORTEP drawing of [RhCl(COD)(**1**,κP)], (S_a,R_C,R_C)-**4b**.

Table 3. Selected Bond Lengths (Å) and Angles (deg) for (S_a,R_C,R_C)-4b

Rh−P	2.2481(7)	Rh−Cl	2.3499(8)
Rh−C(37)	2.137(3)	Rh−C(38)	2.124(3)
Rh−C(41)	2.270(3)	Rh−C(42)	2.243(3)
Cl−Rh−C(37)	161.04(8)	Cl−Rh−C(38)	159.89(8)
Cl−Rh−C(41)	93.05(9)	Cl−Rh−C(42)	88.84(9)
P−Rh−C(41)	169.68(9)	P−Rh−C(42)	155.27(9)
P−Rh−C(37)	94.22(8)	P−Rh−C(38)	94.28(9)
P−Rh−Cl	88.53(3)		

Scheme 4

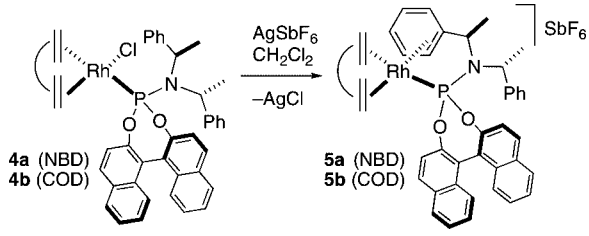

the NBD analogue **4a**, which reflects the stronger bonding (and larger *trans* influence) of 1,5-cyclooctadiene as compared to norbornadiene. X-ray diffraction studies of **4a** (Figure 2, Table 2) and **4b** (Figure 3, Table 3) are informative as to the electronic and steric features of phosphoramidite **1**. In both complexes, the square-planar coordination of the Rh atom is only slightly distorted toward tetrahedral, the centroids of the double bonds and the Rh, P, and Cl atoms lying within ±0.1 and ±0.09 Å from their least-squares plane for **4a** and **4b**, respectively. The diolefin bonding is markedly asymmetric in the norbornadiene derivative **4a**, which features an average rhodium−olefin bond length of 2.25 Å *trans* to P, that is, 0.16 Å longer than the average Rh−C bond *trans* to Cl (2.09 Å). The latter value is close to those observed for $[Rh(NBD)Cl]_2$ and $[Rh(COD)Cl]_2$.[29,30] The phosphoramidite ligand exerts a smaller *trans* influence in the COD complexes, as indicated by **4b** and [RhCl(PPh_3)(COD)], which show Δ(Rh−C) of 0.126 and 0.113 Å, respectively.[31]

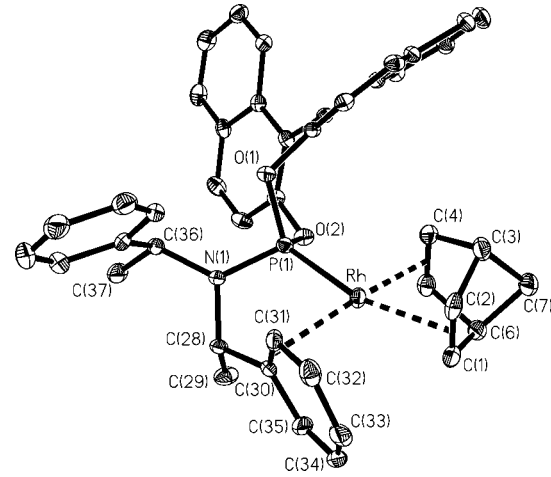

Figure 4. ORTEP drawing of the [Rh(NBD)(1,2-η-Ph-**1**,κP)]$^+$ cation, (R_a,S_C,S_C)-**5a**.

Complexes **4a** and **4b** feature shorter Rh−P distances than their PPh_3 analogues. Thus, the Rh−P distances are 2.2183(7) and 2.307 (1) Å in **4a** and in [RhCl(PPh_3)(NBD)], respectively.[31] This probably reflects the increase of π-acidity and of *s*-character of the phosphorus lone pair as the electronegativity of the P-substituents is increased on going from carbon in PPh_3 to nitrogen and oxygen in ligand **1**. The Rh−P distances in **4a** (and in **4b**) are shorter than those found in some highly crowded $[Rh(COD)(L)_2]^+$ cations (2.275−2.286 Å)[32] (L = phosphoramidite) and are close to that (2.237(2) Å) of a cationic complex containing a P,N-bidentate aminophosphoramidite.[33]

Cationic Rh(I) Complexes. The neutral complexes **4a** and **4b** react with $AgSbF_6$ to give the cationic derivatives [Rh(NBD)(1,2-η-Ph-**1**-κP)]$^+$ (**5a**) and [Rh(COD)(1,2-η-Ph-**1**-κP)]$^+$ (**5b**) as a single diastereoisomer (Scheme 4). This is indicated by the disappearance of the signals of **4a** (or **4b**) in the ^{31}P spectra of reaction solutions in CD_2Cl_2, which is accompanied by the appearance of a doublet at lower field at δ 138.9 ($^1J_{Rh,P}$ = 259 Hz) (for **5b**: δ 140.4, $^1J_{Rh,P}$ = 224 Hz). Surprisingly, the $^1J_{Rh,P}$ coupling constants are smaller in **5a** and **5b** than in **4a** and **4b**. Complexes **5a** and **5b** were isolated in high yield and fully characterized by NMR spectroscopy (see below). In the case of **5a**, an X-ray structure confirmed the η^2-coordination of one phenethyl group. Unfortunately, no crystals of **5b** were obtained.

Crystals of [Rh(NBD)(1,2-η-Ph-**1**-κP)]SbF_6 (**5a**) were grown from a MeOH solution of (S_a,R_C,R_C+R_a,S_C,S_C)-**5a**. The crystal studied features a complex cation containing the (S_a,R_C,R_C)-**1** ligand (Figure 4, Table 4), along with the $[SbF_6]^-$ counterion. Despite the racemic ligand (S_a,R_C,R_C+R_a,S_C,S_C)-**1** being used, the complex crystallized in the chiral $P2_12_12_1$ space group, and the absolute structure of the ligand in the crystal chosen is S_a,R_C,R_C, as determined by the Flack parameter.[34] The most significant structural feature is the contact between rhodium and the *ipso* (C(30), 2.405(3) Å) and *ortho* (C(31), 2.457(4) Å) carbon atoms of one phenyl ring, which indicates a weak, asymmetric bonding interaction and completes a moderately distorted square-planar structure. The C−C distances in the phenyl ring indicate a small distortion of the 1,2-η-bound phenyl,

(29) (a) Englert, U.; Koelle, U. *Z. Kristallogr.* **1996**, *211*, 64. (b) De Ridder, D. J. A.; Imhoff, P. *Acta Crystallogr., Sect. C: Cryst. Struct. Commun.* **1994**, *C50*, 1569.

(30) Takenaka, Y.; Osakada, K. *Bull. Chem. Soc. Jpn.* **2000**, *73*, 129.

(31) Horn, Q. L.; Jones, D. S.; Evans, R. N.; Ogle, C. A.; Masterman, T. C. *Acta Crystallogr., Sect. E: Struct. Rep. Online* **2002**, *58*, m51, DOI: 10.1107/S1600536802000077.

(32) Reetz, M. T.; Ma, J.-; Goddard, R. *Angew. Chem., Int. Ed. Engl.* **2005**, *44*, 412. (a) Hu, A.-G.; Fu, Y.; Xie, J.-H.; Zhou, H.; Wang, L.-X.; Zhou, Q.-L. *Angew. Chem., Int. Ed.* **2002**, *41*, 2348.

(33) Arena, C. G.; Pattacini, R. *J. Mol. Catal. A* **2004**, *222*, 47.

(34) As this absolute configuration is opposite that of **4a**, the ligands depicted in Figures 2 and 4 are enantiomers.

Table 4. Selected Bond Lengths (Å) and Angles (deg) for (S_a,R_C,R_C+R_a,S_C,S_C)-5a

Rh−P	2.1908(9)	Rh···C(35)	2.927(4)
Rh−C(1)	2.320(4)	Rh−C(2)	2.305(3)
Rh−C(4)	2.106(4)	Rh−C(5)	2.092(3)
Rh−C(30)	2.405(3)	Rh−C(31)	2.457(4)
C(30)−C(31)	1.401(5)	C(31)−C(32)	1.395(5)
C(32)−C(33)	1.381(6)	C(33)−C(34)	1.366(7)
C(34)−C(35)	1.396(6)	C(30)−C(35)	1.406(5)
P−Rh−C(1)	161.65(10)	P−Rh−C(2)	152.85(11)
P−Rh−C(4)	94.09(11)	P−Rh−C(5)	98.08(11)
P−Rh−C(30)	79.85(8)	P−Rh−C(31)	88.61(8)
C(4)−Rh-C(30)	172.41(14)	C(5)−Rh-C(31)	167.22(14)
C(1)−Rh-C(30)	107.78(12)	C(2)−Rh-C(30)	122.18(13)
C(1)−Rh-C(31)	107.02(12)	C(2)−Rh-C(31)	102.07(13)

Table 5. ^{13}C NMR Spectroscopic Data for Coordinated and Uncoordinated (in parentheses) Phenyl Rings of [Rh(NBD)(1,2-η-Ph-1-κP)]$^+$ (5a), [Rh(COD)(1,2-η-Ph-1-κP)]$^+$ (5b), and [Rh(1-κP)(η^6-Ph-1,κP)]$^+$ (6)[a]

	5a	5b	6	7[b]
C(1) *ipso*	128.7 (138.9)	139.3 (138.4)	112.4 [−26] [a]	106.6
C(2) *ortho*	103.7 (128.1)	100.1 (128.0)	102.9 [−25]	80.6
C(3) *meta*	135.5(128.8)	139.7 (128.6)	114.2 [−14]	97.8
C(4) *para*	128.3 (128.2)	128.2 (128.2)	98.4 [−30]	95.0
C(5)*meta′*	131.4 (128.8)	134.2 (128.6)	103.0 [−26]	104.9
C(6) *ortho′*	128.0 (128.1)	130.2 (128.0)	109.0 [−19]	81.0

[a] Values in brackets are coordination chemical shifts calculated on the basis of the average value of the corresponding free C atom in **5a** and **5b**. [b] From ref 10a.

with a long C(30)−C(31) bond distance (Table 4). However, the overall expansion of the ring is very small, the average C−C distance (1.391(15) Å) being close to that of the noncoordinated phenyl ring (1.383(14) Å). Starting from the long Rh−C distances, several observations suggest that the η^2-phenyl−metal interaction is weak. Thus, the phenyl ring shows only modest deviations from planarity, the largest ones being 0.037 Å (away from Rh) and −0.030 Å (toward Rh) for C(30) and C(33), respectively. The pyramidalization of the *ipso* carbon atom C(30) is insignificant (the sum of the C−C−C angles is 358.8°). The largest distortion in the phenethyl group is the displacement of the exocyclic C(28) by 0.44 Å from the phenyl plane.

The Rh−P bond distance is slightly shorter in **5a** than in the neutral precursor **4a** (2.1908(9) vs 2.2183(7) Å, respectively), which can be explained by the chelate effect. The strengthening of the Rh−P bond in **5a** is reflected in the lengthening of the *trans*-lying Rh−C(1) and Rh−C(2) bonds (2.320(4) and 2.305(3) Å) as compared to those of **4a** (2.261(3) and 2.240(3) Å, respectively). Interestingly, the $^1J_{Rh,P}$ coupling constant does not reflect this trend, as it is lower in **5a** and in **4a** (the same applies for the COD analogues **4b** and **5b**). This is most probably due to the angular strain imposed by the chelate (the average P−Rh-(1,2-η-phenyl) angle is 84°), which reduces the *s*-character of the Rh−P bond and hence the $^1J_{Rh,P}$ coupling constant.[35]

The X-ray structure of **5a** shows that the 1,2-η-Ph−metal interaction is unsymmetrical, with the *ipso* carbon closer to rhodium than the *ortho* carbon. However, the opposite trend would be expected on the basis of ^{13}C NMR spectral data, which show the largest coordination shift $\Delta\delta$ for the *ortho* C atom. This reminds one that several factors combine to determine the ^{13}C NMR chemical shift (including steric crowding), which makes structural interpretations based only on $\delta(^{13}C)$ values rather unreliable. To further assess this point, we attempted to crystallize the COD analogue **5b**. However, such attempts yielded a product of COD loss instead (see below).

The 1,2-η-arene interaction in **5a** is rare but not unprecedented for rhodium complexes. The formally three-coordinate [Rh(P-Ph$_3$)$_3$]$^+$ reaches a 16-electron count by 1,2-η-Ph-coordination of a PPh$_3$ phenyl ring.[36] Owing to the angular strain of the four-membered ring, the Rh−C$_{ipso}$ and Rh−C$_{ortho}$ distances (2.48(2) and 2.62(2) Å) are much longer than in **5a**. Rhodium(II) binuclear complexes feature even weaker 1,2-η-arene interactions involving the labile axial coordination site, with Rh−C distances in the range 2.598(7)−2.770(7) Å.[37] Interestingly, severely crowded olefin complexes of rhodium(I) exhibit Rh(I)−olefin bonds with Rh−C distances in the range 2.337(4)−2.451(4), which are close to the values found in **5a**.[38]

NMR Spectroscopic Studies of 5a and 5b. The ^{13}C NMR signals of the free and coordinated benzyl fragments were assigned by a combination of 2D NMR spectroscopic techniques. The line widths for the majority of proton resonances in the room-temperature ^{1}H NMR spectra of **5a** and **5b** indicate a dynamic behavior on the NMR time scale, but the exchange process is slow at −90 °C, and the signals sharpen sufficiently to measure one-bond and long-range ^{13}C−^{1}H correlations. No Rh−C(arene) coupling was observed, though. The signals of the two diastereotopic N−CH(Me)Ph methine protons and carbons were assigned by ^{31}P−^{1}H HMQC correlation and were connected to the corresponding Rh-bound and free phenyl rings with the help of ^{1}H,^{1}H-COSY.[39] One of the N−CH(Me)Ph phenyls is freely rotating and features normal aromatic ^{13}C chemical shifts. In contrast, the second N−CH(Me)Ph phenyl ring contains six inequivalent C atoms,[40] and one *ortho* C atom resonates at lower frequency as compared to the freely rotating phenyl ring. The coordination shifts ($\Delta\delta$) of this *ortho* C atom are −24.4 for **5a** and −27.9 ppm for **5b**, respectively (Table 5). Interestingly, the signal of the *ipso* C atom is shifted to low frequency in the NBD derivative **5a** ($\Delta\delta$ = −10.2 ppm) but is nearly unperturbed in the COD analogue **5b**.

Overall, these data suggest a modest to weak π-olefin-type interaction between rhodium and one phenyl ring,[41] but their interpretation is not conclusive in view of the different NMR spectroscopic patterns observed for **5a** and **5b** and in the absence of X-ray data for the latter complex. On the basis of only the ^{13}C chemical shifts of the *ortho* and *ipso* carbons, the bonding asymmetry seems to be larger in the COD derivative **5b** than in the NBD complex **5a**. This might reflect the larger steric crowding in **5b**, which might also explain the difference in stability of these complexes (see below).

(35) Pregosin, P. S.; Kunz, R. W. *^{31}P and ^{13}C NMR of Transition Metal Phosphine Complexes*. In *NMR Basic Principles and Progress*; Diehl, P., Fluck, E., Kosfeld, R. Eds.; Springer: Berlin, 1979; p 16.

(36) Yared, Y. W.; Miles, S. L.; Bau, R.; Reed, C. A. *J. Am. Chem. Soc.* **1977**, *97*, 7076.

(37) Cotton, F. A.; Dikarev, E. V.; Petrukhina, M. A.; Stiriba, S. *Polyhedron* **2000**, *19*, 1829.

(38) Deblon, S.; Rüegger, H.; Schönberg, H.; Loss, S.; Gramlich, V.; Grützmacher, H. *New J. Chem.* **2001**, *25*, 83.

(39) The ^{13}C NMR signal of the C$_{ortho}$ at δ 103.7 in **5a** (100.1 for **5b**) was identified by an HMQC experiment from the one-bond interaction to the *ortho* proton at δ 6.47 (**5a**) and 6.56 (**5b**), respectively. Analogously, C$_{ipso}$ was found to resonate at δ 128.7 in **5a** (139.3 for **5b**), as indicated by the three-bond interactions to the protons of the methyl group in PNC(C*H*$_3$)H and by the two-bond interactions to PNC*H* in an HMBC experiment.

(40) The spectral pattern of the methine protons further suggests that the two N−CH(Me)Ph groups have different conformations. That belonging to the "frozen", η^2-complexed moiety appears as a doublet of quartets (δ = 4.07, $^3J_{P,H}$ = 41 Hz for **5a** and δ = 4.08, $^3J_{P,H}$ = 45 Hz for **5b**), whereas that of the dangling N−CH(Me)Ph group is observed as a multiplet (δ = 4.51, $^3J_{P,H}$ = 6 Hz for **5a** and δ = 4.58, $^3J_{P,H}$ = 7 Hz for **5b**).

(41) Mann, B. E.; Taylor, B. F. B. *13C-NMR Data for Organometallic Compounds*; Academic Press: London, 1981.

Scheme 5

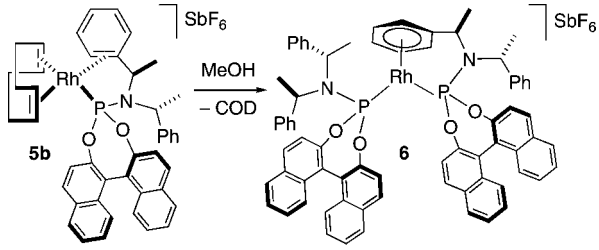

[Rh(1-κP)(η^6-Ph-1-κP)]SbF$_6$ (6). When racemic (S_a,R_C,R_C+ R_a,S_C,S_C)-[Rh(COD)(1,2-η-Ph-**1**-κP)]$^+$ (*rac*-**5b**) is dissolved in polar, coordinating solvents such as methanol, ligand rearrangement takes place within a few days to give [Rh(**1**-κP)(η^6-Ph-**1**-κP)]SbF$_6$ (**6**) as yellow-orange crystals of X-ray quality (Scheme 5). In contrast, the NBD derivative **5a** is indefinitely stable in MeOH solution. To explain this behavior, we note that COD forms a less strained chelate ring with better orbital overlap, and hence exerts a larger *trans* influence than NBD. Indications thereof are the smaller $J_{Rh,P}$ coupling constant of the COD derivative **5b** (224 Hz) as compared to NBD complex **5a** (259 Hz) and the longer Rh−P bond observed in the neutral COD analogues **4b** (2.2481(7) Å) as compared to the NBD complex **4a** (2.2183(7) Å). Therefore, the η^2-interaction is weaker in the COD derivative **5b** than in the NBD analogue **5a** (as confirmed by the coordination chemical shifts in Table 5), which may favor the dissociation of the phosphoramidite aryl and the reaction with methanol in the former.

In complex **6**, which was fully characterized, one of the phosphoramidites is monodentate, whereas the second one features the η^6-coordination of one phenyl group additionally to P-coordination. The η^6-aryl coordination is supported by ^{31}P, ^{1}H, and ^{13}C NMR spectroscopy, as well as by an X-ray study. The room-temperature ^{31}P NMR spectrum in CD_2Cl_2 features a broad doublet at δ 146.9 ($^1J_{Rh,P}$ = 322 Hz). The equivalence of the P atoms is indicative of fast arene exchange. Upon lowering the temperature, the signal broadens and a static spectrum is obtained at −90 °C. This shows two well-resolved doublets of doublets in the ^{31}P NMR spectrum at 150.5 ($^1J_{Rh,P}$ = 314 Hz, $^2J_{P,P}$ = 21 Hz) and 147.3 ($^1J_{Rh,P}$ = 327 Hz, $^2J_{P,P}$ = 21 Hz), which correspond to the monodentate (**1**,κP) and to the η^6-bound (η^6-Ph-**1**,κP) ligands, respectively. All of the ^{13}C NMR signals of the coordinated phenyl ring were assigned, but severe overlap in the ^{1}H NMR spectrum precluded the full signal assignment for the carbon atoms of the uncoordinated phenyl rings. The ^{13}C NMR resonances of the η^6-phenyl ring were found at lower frequency as compared to those of the uncoordinated one. No Rh−C(arene) coupling was observed. The estimated coordination chemical shifts $\Delta\delta$ (based on the average of the corresponding signals of the free phenyl groups of **5a** and **5b**, Table 5) are in the typical range between −14 and −26 observed for other η^6-arene Rh(I) complexes.[42]

The solid-state structure of **6** (prepared from racemic **5b**) was unambiguously determined by X-ray diffraction (Figure 5, Table 6). The asymmetric unit contains two crystallographically independent cations **6** and two [SbF$_6$]$^-$ anions with undistinguishable metrical parameters. As both ligands **1** have the same absolute configuration in each cation, only the *l* diastereoisomer is formed as a pair of enantiomers (S_a,S_a,R_C,R_C,R_C,R_C)-[Rh(**1**-κP)(η^6-Ph-**1**-κP)]$^+$ and (R_a,R_a,S_C,S_C,S_C,S_C)-[Rh(**1**-κP)(η^6-Ph-**1**-κP)]$^+$. Only one of the crystallographically independent enantiomers is discussed (Table 6). Figure 5 shows S_a,S_a,R_C,R_C,R_C,R_C-**6**.

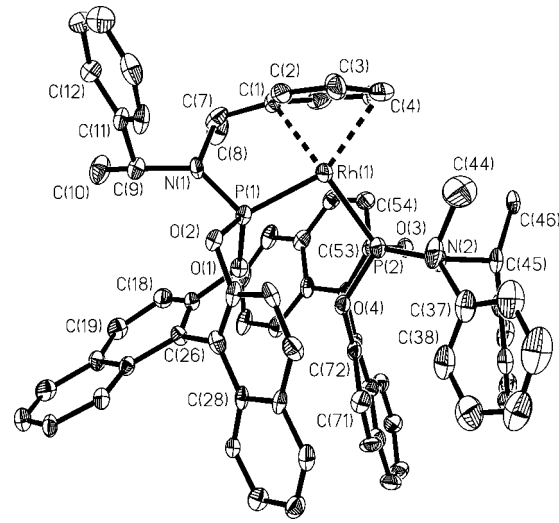

Figure 5. ORTEP drawing of the (S_a,S_a,R_C,R_C,R_C,R_C)-[Rh(**1**-κP)(η^6-Ph-**1**-κP)]$^+$ cation, **6**.

Table 6. Selected Bond Lengths (Å) and Angles (deg) for (S_a,S_a,R_C,R_C,R_C,R_C)-[Rh(1-κP)(η^6-Ph-1-κP)]$^+$ (6)

Rh(1)−P(1)	2.177(3)	Rh(1)−P(2)	2.217(3)
Rh(1)−C(1)	2.198(10)	Rh(1)−C(4)	2.370(11)
Rh(1)−C(2)	2.338(11)	Rh(1)−C(5)	2.394(12)
Rh(1)−C(3)	2.408(11)	Rh(1)−C(6)	2.252(11)
P(1)−Rh(1)−C(1)	81.9(3)	P(2)−Rh(1)−C(1)	158.7(3)
P(1)−Rh(1)−C(4)	150.6(3)	P(2)−Rh(1)−C(4)	109.7(3)
P(1)−Rh(1)−P(2)	98.03(11)		

The coordination sphere of rhodium is typical of half-sandwich d^8 complexes of general type [ML$_2$(arene)]$^{n+}$, in which the metal, both L ligands, and the centroid of the arene are nearly coplanar.[22] The arene ring is roughly perpendicular (82.6(3)°) to the plane of the ML$_2$ fragment, the small deviation from the ideal value of 90° being attributable to chelation, and the conformation of the η^6-arene is such that the ML$_2$ unit eclipses C(1) and C(4). We have chosen to draw **6** as a square-planar complex in Figure 5 to emphasize this aspect (see below). The coordinated phenyl ring is nonplanar, with C(1) and C(4) displaced from the mean square plane by 0.051(8) and 0.055(8) Å toward rhodium, whereas C(2), C(3), C(5), and C(6) are pushed away by 0.013(8)−0.040(8) Å. Although this contributes to releasing the steric strain of the chelate in the present case, such a distortion has a purely electronic origin and is general for d^8 complexes of the type [M(η^6-arene)(L)$_2$]$^{n+}$ that feature the same "eclipsed" conformation as **6**.[22]

The η^6-arene coordination to rhodium(I) is a well-known structural motif, and several examples thereof have been reported.[22,23] The closest analogue of **6** is [Rh(hydroquinone)(P(OPh)$_3$)$_2$]$^+$, which has been developed as a unit for self-assembly directed by hydrogen bonding and $\pi-\pi$ stacking.[43] This complex features a short Rh−P distance (average 2.18 Å), whereas the average Rh−arene (2.33 Å) is normal for Rh(I) η^6-arene complexes, as in the closely related species [Rh(L^1,κP)(η^6-

(42) Aresta, M.; Quaranta, E.; Albinati, A. *Organometallics* **1993**, *12*, 2032.

(43) Son, S. U.; Rheingold, J. A.; Carpenter, G. B.; Czech, P. T.; Sweigart, D. A. *Organometallics* **2006**, *25*, 5276.

Chart 3

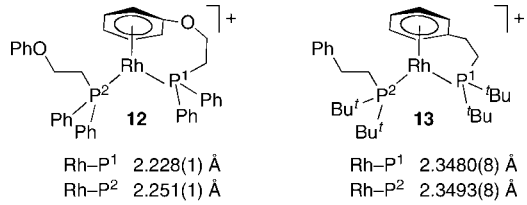

$L^1,\kappa P)]^+$ ($L^1 = Ph_2PCH_2CH_2OPh$) (**12**)[44] and $[Rh(L^2,\kappa P)(\eta^6$-$L^2,\kappa P)]^+$ ($L^2 = {}^tBu_2PCH_2CH_2Ph$) (**13**) (Chart 3).[45]

The Rh−P distances suggest that the Rh−P bond becomes weaker on going from **6** to **12** and **13** (Table 6, Chart 3). As this should imply that the Rh−arene bond strength increases in the same order, it is tempting to correlate these data with the solution behavior of **6**, **12**, and **13**. In fact, the phosphoramidite derivative **6** is fluxional in CD_2Cl_2 at room temperature, whereas no arene exchange is observed for **13** under the same conditions.[45] Complex **12** has an intermediate behavior and is fluxional in donor solvents (THF) above 208 K.[44] Therefore, the Rh−P distance seems to correlate nicely with the *trans* influence of the P donor, as the complex with the shortest Rh−P bonds is the most labile complex in the series. Unfortunately, the average rhodium−arene distance is the same (2.33 Å) in all complexes and is, therefore, not diagnostic as to the strength of the Rh−arene bond. The lability of the arene in **6** is intriguing, as π-arene complexes of rhodium(I) have been early proposed to play a role in stabilizing catalysis intermediates.[46] The origin of arene distortion, and of its lability, is discussed in the next section.

η^6-Arene Coordination in d^8 and d^6 Complexes. Deviations from planarity of the type described above are typical of η^6-arenes in d^8 complexes of the type $[ML_2(\eta^6$-arene$)]^{n+}$ in which the ML_2 plane bisects two C−C bonds of the arene, as it applies for **6**. It has been thoroughly demonstrated that the origin of this distortion is electronic in nature.[22] To understand this, one has to consider the orbitals of the metal(η^6-arene) fragment, which result from the antibonding combination of d_{xz} (b_1) and d_{yz} (b_2) with the arene orbitals (Figure 6). The b_1 and b_2 orbitals are kept at low energy by the interaction with the p_x and p_y metal orbitals in a bonding (less antibonding) way with respect to the arene orbitals shown.[22] In the conformation observed for **6** (Figure 5), the (unoccupied) b_2 orbital is used to bind to the L_2 ligand set. Therefore, b_1 is nonbonding with respect to L_2 but antibonding between metal and arene, and in particular between the metal and the C atoms outside the ML_2 plane (right side of Figure 6). As b_1 is occupied (HOMO) in a d^8 metal complex, the C atoms that lie outside the ML_2 plane are displaced away from the metal to decrease the four-electron repulsion and lower the energy, as observed for C(2), C(3), C(5), and C(6) in **6**.

An important consequence is that, because the M−arene bond encompasses six bonding and two antibonding electrons, the total bond border between the arene ring in a d^8 $[M(\eta^6$-arene$)(L)_2]$ complex is 2, and the η^6-arene acts as a four-electron donor. In contrast, in the d^6 complexes $[M(\eta^6$-arene$)(L)_3]^{n+}$,

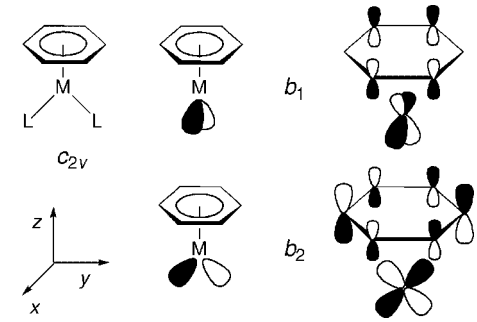

Figure 6. Selected orbitals of the metal(η^6-arene) fragment.

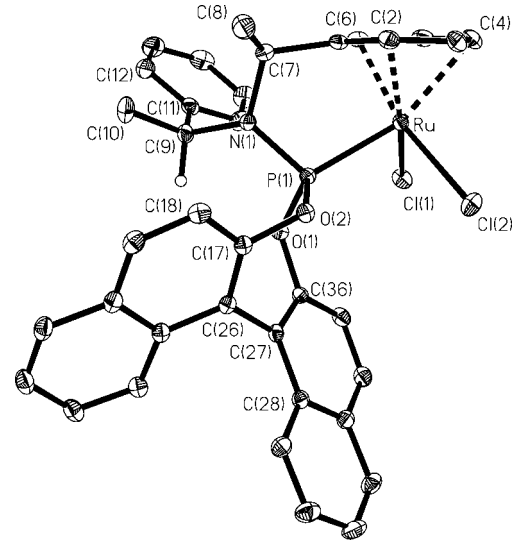

Figure 7. ORTEP drawing of $[RuCl_2(\eta^6$-Ph-**1**,$\kappa P)]$, (S_a,R_c,R_c)-**7**.

Scheme 6

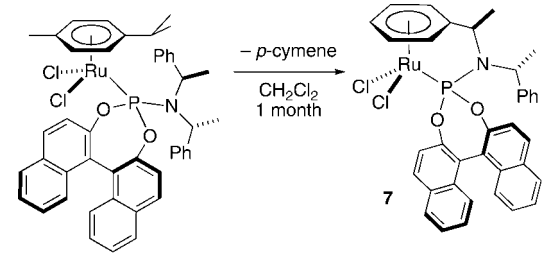

the metal−arene antibonding orbital b_1 is empty, and the arene acts a six-electron donor, which is expected to result in a stronger metal−carbon bond. Thus, for the sake of comparison with the above η^2- and η^6-arene d^8 complexes, in which the arene acts as a two- and four-electron donor, respectively, we determined the structure of the previously reported complex $[RuCl_2(\eta^6$-Ph-**1**,$\kappa P)]$ (**7**) (Figure 7).

$[RuCl_2(\eta^6$-Ph-1,κP)] (7). In a previous article, we have shown that $[RuCl_2(p$-cymene$)($**1**,$\kappa P)]$ spontaneously loses *p*-cymene to give $[RuCl_2(\eta^6$-Ph-**1**,$\kappa P)]$ (**7**), in which the phosphoramidite acts overall as an eight-electron donor (Scheme 6).[10a] This reaction represents a convenient synthetic pathway to chiral ruthenium(II) complexes containing a tethered arene.[47] The crystal structure of **7** confirms the previous formulation based on solution NMR spectroscopic studies and allows a comparison with $[Rh($**1**,$\kappa P)(\eta^6$-Ph-**1**,$\kappa P)]^+$ (**6**). The coordination

(44) Singewald, E. T.; Shi, X.; Mirkin, C. A.; Schofer, S. J.; Stern, C. L. *Organometallics.* **1996**, *15*, 3062.

(45) Canepa, G.; Brandt, C. D.; Ilg, K.; Wolf, J.; Werner, H. *Chem.−Eur. J.* **2003**, *9*, 2502.

(46) Selected papers:(a) Halpern, J.; Riley, D. P.; Chan, A. S. C.; Pluth, J. J. *J. Am. Chem. Soc.* **1977**, *99*, 8055. (b) Townsend, J. M.; Blount, J. F. *Inorg. Chem.* **1981**, *20*, 269. (c) Slone, C. S.; Mirkin, C. A.; Yap, G. P. A.; Guzei, I. A.; Rheingold, A. L. *J. Am. CHem. Soc.* **1997**, *119*, 10743. (d) Gridnev, I. D.; Fan, C.; Pringle, P. G. *Chem. Commun.* **2007**, 1319.

(47) For a review, see:(a) Adams, J. R.; Bennett, M. A. *Adv. Organomet. Chem.* **2006**, *54*, 293.

Table 7. Selected Bond Lengths (Å) and Angles (deg) for (S_a,R_C,R_C+R_a,S_C,S_C)-[$RuCl_2(\eta^6$-Ph-1,κP)]$^+$ (7)

Ru−C(1)	2.123(2)	Ru−C(4)	2.276(2)
Ru−C(2)	2.207(2)	Ru−C(5)	2.239(2)
Ru−C(3)	2.218(2)	Ru−C(6)	2.173(2)
Ru−Cl(1)	2.3894(6)	Ru−Cl(2)	2.4010(6)
Ru−P(1)	2.2622(6)		
P(1)−Ru−C(2)	95.08(7)	P(1)−Ru−Cl(1)	89.61(2)
P(1)−Ru−C(4)	159.58(7)	P(1)−Ru(1)−Cl(2)	93.11(2)
P(1)−Ru−C(6)	98.66(7)	Cl(1)−Ru(1)−Cl(2)	89.68(2)
Cl(1)−Ru−C(2)	162.45(7)	Cl(2)−Ru(1)−C(2)	106.89(6)
Cl(1)−Ru−C(4)	105.08(7)	Cl(2)−Ru(1)−C(4)	100.93(7)
Cl(1)−Ru−C(6)	94.05(7)	Cl(2)−Ru(1)−C(6)	167.67(7)

Table 8. Average Metal−Carbon Bond Lenghths (M−C) and Largest Difference within a Group (Δ_{max}) (Å)

	2	**3**	**5a**	**6** [a]	**7**
metal/bond	d^6/η^2	d^8/η^2	d^8/η^2	d^8/η^6	d^6/η^6
M−C	2.38	2.46	2.43	2.33	2.21
Δ_{max}	0.01	0.10	0.05	0.21	0.15
M−P	2.28	2.26	2.19	2.20 [b]	2.26

[a] Average of all six M−C distances. [b] Average of Rh(1)−P(1) and Rh(1)−P(2).

of ruthenium is pseudo-octahedral, with C(2), C(4), and C(6) staggered with respect to the P and Cl atoms (Table 7). The Ru−Cl bond lengths, 2.3894(6) and 2.4010(6) Å, differ only slightly from those of the starting complex [$RuCl_2$(*p*-cymene)(**1**,κP)] (2.387(3) and 2.405(3) Å),[10a] but the Ru−P bond is significantly shortened (2.2622(6) vs 2.317(3) Å) due to the chelate effect.

The distances to the aromatic ring are normal, with an average of 2.21 Å vs 2.20 Å in [$RuCl_2$(*p*-cymene)(**1**,κP)]. However, they are spread because of the strain imposed by chelation, with the shortest one involving the *ipso* C atom C(1). Although many Ru(II) complexes with a two-atom tether between a P donor and an η^6-arene have been structurally characterized,[48] **7** is, to the best of our knowledge, the first one containing a phosphoramidite ligand. The closest analogue is the phosphite derivative [$RuCl_2(\eta^6$-*p*-cymene)(P(OPh)$_3$)], which features similar Ru−P (2.2642(8) Å), Ru−Cl (2.3992(8), 2.4022(8) Å), and Ru−C distances (average 2.21 Å).[49]

Electron Count, M−C Distances, and Fluxionality. Finally, we discuss here the general relationships between hapticity, electron count, average M−C and M−P bonding distances (Table 8), and solution behavior of **2**, **3a**, **5a**, **6**, and **7**. The comparison of the M−C distances is not straightforward because (a) the metals involved have different atomic radii and (b) the bonding is unsymmetrical. However, the spread of the M−P distances over all these species (0.09 Å) is much smaller than that of the average M−C bond lengths (0.25 Å). Therefore, we conclude that hapticity and electron configuration affect the M−C distances more than the atomic radius. Within the limits of this approximation, the comparison shows a steady decrease of the M−C distance as the number of electrons involved in the bonding increases. The weakest metal−aryl bond is found for the η^2-aryl coordination in the d^8 complexes **3** and **5a**, that is, for an arene that acts as a two-electron donor. In **6**, where the arene acts in fact as a four-electron donor, we observe the intermediate average M−C distance, whereas **7**, in which the η^6-arene is a six-electron donor, gives the shortest M−C bonds.

With the usual caveat concerning the comparison of thermodynamic and kinetic phenomena, it is intriguing to notice that the NMR spectroscopic behavior in CD_2Cl_2 qualitatively follows the trends of the M−C distances. The d^8 species **3**, **5a**, and **6** are highly dynamic in CD_2Cl_2 at room temperature, and cooling to −90 °C is required to obtain resolved ^{13}C NMR spectra, whereas [$RuCl_2(\eta^6$-Ph-**1**-κP)]$^+$ (**7**) gives resolved spectra at room temperature.[10a] It should be noted that the d^6 complex [RuCl(η^6-*p*-cymene)(1,2-η-Ph-P*-κP)]PF_6 (**2**) gives a resolved ^{13}C NMR spectrum at −20 °C and is thus less fluxional than the d^8 η^2-phenyl derivatives, which must be cooled to −90 °C to give a static ^{13}C NMR spectrum.[10b] The reason for this difference seems to go beyond kinetic factors (the inert nature of octahedral d^6 complexes), as indicated by the observation that the reduced fluxionality of **2** correlates nicely with its shorter M−C distances (2.38 Å) as compared to **3** and **5a** (2.43−2.46 Å). DFT calculations[28] show that the η^2-phenyl interaction is considerably stronger in **2** (30 kJ/mol) than in **3** (13 kJ/mol) and, thus, quantitatively support our observation. Furthermore, the weak bond in the η^2-arene d^8 complexes **3** and **5a** is in agreement with the easy arene displacement observed for these complexes. On the basis of the above observations, one might speculate that d^8 complexes featuring metal−π-aryl interactions should be more labile—and hence potentially faster catalysts—than their d^6 analogues.

Conclusion

Although phosphoramidite ligands are generally considered *a priori* as monodentate chiral ligands, they are capable of secondary interactions with d^6 and d^8 metals when they contain benzyl substituents at nitrogen. Such derivatives can give coordination of the arene with different hapticity (η^2 or η^6), thus behaving as donors of a total of two, four, six, or eight electrons. Therefore, care should be taken when monodentate behavior is taken for granted without supporting evidence. In particular, this is the case of catalytic reactions, whose cycles involve in general several different metal complexes. The new bonding modes should (a) prove useful in designing new ligands that can give secondary interactions of variable strength and (b) contribute to an understanding of the mechanisms of existing catalytic reactions. Further, the present study shows that the spectroscopic features of the complexes reported above are not all well understood. Therefore, their diagnostic value for the assessment of arene coordination is limited, and X-ray structural studies are still pivotal. We are currently working on the synthesis and application in catalysis of d^8 complexes containing chiral phosphoramidites that feature η^2- and η^6-arene coordination.

Experimental Part

General Comments. Unless otherwise stated, the absolute configuration of ligand **1** is S_a,R_C,R_C. Reactions with air- or moisture-sensitive materials were carried out under an argon atmosphere using Schlenk techniques or in a glovebox under purified nitrogen. (*R*)-(−)-Bis(1-phenylethyl)amine hydrochloride was obtained from Aldrich. *S*-(−)-1,1′-Bi(2-naphthol), [$Pd(C_3H_5)Cl]_2$, and phosphorus trichloride were purchased from Fluka. [Rh(COD)Cl]$_2$

(48) Selected recent examples:(a) Therrien, B.; Ward, T. R.; Pilkington, M.; Hoffmann, C.; Gilardoni, F.; Weber, J. *Organometallics* **1998**, *17*, 330. (b) Abele, A.; Wursche, R.; Klinga, M.; Rieger, B. *J. Mol. Catal. A: Chem.* **2000**, *23*, 160. (c) Bennett, M. A.; Edwards, A. J.; Harper, J. R.; Khimyak, T.; Willis, A. C. *J. Organomet. Chem.* **2001**, *629*, 7. (d) Jung, S.; Ilg, K.; Brandt, C. D.; Wolf, J.; Werner, H. *J. Chem. Soc., Dalton Trans.* **2002**, 318. (e) Hermatschweiler, R.; Pregosin, P. S.; Albinati, A.; Rizzato, S. *Inorg. Chim. Acta* **2003**, *354*, 90. (f) Umezawa-Vizzini, K.; Guzman-Jimenez, I. Y.; Whitmire, K. H.; Lee, T. R. *Organometallics* **2003**, *22*, 3059. (g) Hannedouche, J.; Clarkson, G. J.; Wills, M. *J. Am. Chem. Soc.* **2004**, *126*, 986. (h) Faller, J. W.; Fontaine, P. P. *J. Organomet. Chem.* **2007**, *692*, 1110.

(49) Hodson, E.; Simpson, S. J. *Polyhedron* **2004**, *23*, 2695.

and $[Rh(NBD)Cl]_2$ were obtained from Pressure Chemicals and Alfa Aesar, respectively. Silver hexafluoroantimonate was purchased from Acros. PCl_3 was distilled immediately before use. NEt_3 was freshly distilled on CaH_2. All other commercially available reagents were used without further purification. Solvents were purified by standard procedures: CH_2Cl_2 and CD_2Cl_2 were distilled from CaH_2. Optical rotations were measured using a Perkin-Elmer 341 polarimeter with a 1 dm cell in $CHCl_3$, unless otherwise stated. Mass spectra were measured by the MS-service (Laboratorium für Organische Chemie, ETH Zürich). The HR MALDI spectra were obtained on a IonSpec Ultima HR MALDI-FT-ICR mass spectrometer at 4.7 T using a DCTB (*trans*-2-[3-(4-*tert*-butylphenyl)-2-methyl-2-propylidene]malononitrile) matrix. Elemental analyses were carried out by the Laboratory of Microelemental Analysis (Laboratorium für Organische Chemie, ETH Zürich). ^1H (700.1, 500.1, and 300.1 MHz), ^{31}P (283.4, 202.5, and 121.5 MHz), and ^{13}C (176.1, 125.8, and 75.5 MHz) spectra were recorded on Bruker Avance 700, 500, and 300 MHz spectrometers, respectively, as CD_2Cl_2 solutions, unless otherwise stated. Chemical shifts δ are quoted in parts per million (ppm) downfield of tetramethylsilane. ^{31}P NMR chemical shifts were referenced externally to 85% H_3PO_4 (δ 0.0). Coupling constants J are given in Hz. Phosphoramidite **1** was prepared in a straightforward manner by a modification of the recently reported one-pot procedure.[50]

Ligand 1. A 100 mL three-necked flask was charged with freshly distilled PCl_3 (0.9865 g, 0.007183 mol) in anhydrous CH_2Cl_2 (12 mL). The solution was cooled to 0 °C, and NEt_3 (5 mL, 3.6344 g, 0.0359 mol) was added dropwise over 1 min to the solution. A solution of (*R,R*)-bis(1-phenylethyl)amine hydrochloride (1.8805 g, 0.007183 mol) in CH_2Cl_2 (30 mL) was slowly added over 30 min to the reaction mixture kept at 0 °C, and CH_2Cl_2 (5 mL) was used to rinse the funnel. After completing the addition, the ice bath was removed, and the resulting suspension was stirred for 90 min at 20 °C. Then, the reaction mixture was cooled to 0 °C, and a solution of (*S*)-binaphthol (2.0568 g, 0.007183 mol) in a mixture of CH_2Cl_2 (25 mL) and NEt_3 (2 mL) was added dropwise over 30 min thereto. The reaction mixture was allowed to warm to 20 °C and stirred overnight, after which H_2O (30 mL) was added. The aqueous phase was extracted once with CH_2Cl_2 (40 mL). The combined organic phases were dried over Na_2SO_4, the salt was removed by filtration, and the solution was evaporated to afford the crude ligand, which was purified by flash chromatography under pressure of argon: R_f 0.4 (3:1 (v/v) pentane/CH_2Cl_2). The solvent was evaporated, and the product was dried under vacuum (0.04 mm) to afford (S_a,R_C,R_C)-*O*,*O*′-[1,1′-binaphthyl-2,2′-diyl]-*N*,*N*′-bis[1-phenylethyl]phosphoramidite, (S_a,R_C,R_C)-**1**, as a white powder. Yield: 3.3661 g, 87%. $[\alpha]_D^{20} = +497$ (c 1.0). ^{31}P NMR (121.49 MHz, C_6D_6): δ 146.2. ^1H NMR (300.13 MHz, C_6D_6): δ 1.70 (d, $^3J_{H,H} = 7.1$, 6 H, CHCH_3), 4.69 (m, $^3J_{H,H} = 7.0$, $^3J_{P,H} = 11.5$, 2 H, CHCH$_3$), 6.96−7.27 (m, 14 H), 7.25 (d, $^3J_{H,H} = 8.7$, 1 H), 7.37 (d, $^3J_{H,H} = 8.6$, 1 H), 7.51−7.70 (m, 4 H), 7.78−7.83 (m, 2 H, arom). Ligand **1** tolerates washing with water in CH_2Cl_2 solution and is stable even without inert gas protection. Less than 10% of ligand oxide (δ_P 11.3) was detected by ^{31}P NMR spectroscopy after exposing a solution of **1** in $CDCl_3$ to the atmosphere for 1 week.

[Pd(η^3-C_3H_5)(1,2-η-Ph-1-κP)]SbF$_6$ (3). A CH_2Cl_2 solution (10 mL) of ligand **1** (0.1079 g, 0.0002 mol) was slowly added dropwise to a CH_2Cl_2 solution (5 mL) of $[Pd(C_3H_5)Cl]_2$ (0.0366 g, 0.0001 mol) over 20 min at room temperature upon stirring. The resulting solution was added to $AgSbF_6$ (0.0687 g, 0.0002 mol), and the resulting slurry was stirred for 2 h. AgCl was filtered off, and the filter was rinsed with CH_2Cl_2 (4 mL). The resulting clear solution was evaporated, and the yellow-green solid was washed with a small amount of diethyl ether (twice) and pentane and dried in air and then under vacuum (0.05 mm). Yield: 0.1753 g, 95%. $[\alpha]_D^{20} = +232$ (c 0.05). Anal. Calcd for $C_{39}H_{35}NO_2F_6PPdSb$: C, 50.76; H, 3.82; N, 1.52. Found: C, 50.60; H, 3.91; N, 1.54. HRMS (MALDI): calcd for $C_{39}H_{35}NO_2PPd$ 686.1435, found 686.1442 $[M - SbF_6]^+$. ^{13}C NMR (125.78 MHz, CD_2Cl_2, −90 °C): δ 19.3 and 19.4 (free NCHCH_3), 23.3 and 23.4 (coord. NCHCH_3), 51.4 (d, $^2J_{P,C} = 26.9$) and 51.5 (d, $^2J_{P,C} = 28.1$) (coord. N$CHCH_3$), 53.9 ($^2J_{P,C} = 7.9$, free N$CHCH_3$), 57.4 (allyl CH_2, *trans* to Ph, major), 59.3 (allyl CH_2, *trans* to Ph, minor), 96.6 (d, $^2J_{P,C} = 39.3$, allyl CH_2, *trans* to P, minor), 97.8 (d, $^2J_{P,C} = 42.5$, allyl CH_2, *trans* to P, major), 113.0 (C_3, *meta* C of coord. Ph, major), 115.2 (C_6, *ortho*′ C of coord. Ph, minor), 117.5 (C^2, *ortho* C of coord. Ph, minor), 120.5, 120.8, 121.0 (C^2, *ortho* C of coord. Ph, major), 121.1 (allyl CH, major), 121.8, 121.9, 122.3 (d, $^3J_{P,C} = 11.8$, allyl CH, minor), 123.0, 123.3, 126.1, 126.2, 126.4, 127.1, 127.2, 128.2, 128.6, 128.8, 129.0, 131.55, 131.62, 131.8 (C^1, C_{ipso} of coord. Ph, major), 131.9, 132.1, 132.16, 132.22, 132.9 (C^1, *ipso* C of coord. Ph, minor), 133.8, 134.2, 134.4, 139.3 (C^1, *ipso* C of free Ph, major + minor), 146.70, 146.74, 146.9 ($J_{P,C}$ 5.0), 147.46, 147.54, 147.6 ($^2J_{P,C} = 10.8$, arom). ^1H NMR (500.23 MHz, CD_2Cl_2, −90 °C): δ 1.48 and 1.54 (br s, 3H, free NCHCH_3), 1.96 (minor) and 2.07 (major) (br s, 3H, coord. NCHCH_3), 2.48 (major + minor) (t, ($J_{H,H} = 13.6$, 1H, allyl CH_2, *trans* to Ph), 2.85 (major) and 3.28 (minor) (m, 1H, allyl CH_2, *trans* to Ph), 3.14 (minor) (t, $J_{H,H} = 14.3$) and 3.95 (major) (t, $J_{H,H} = 14.5$) (1H, allyl CH_2, *trans* to P), 3.39 (major) and 3.65 (minor) (m, 1 H, allyl CH_2, *trans* to P), 4.18 (major and minor), d × q ($^3J_{P,H} = 41.5$, 1 H, coord. NCHCH$_3$), 4.69 (major and minor) (m, 1 H, free NCHCH$_3$), 5.20 (major) 5.48 (minor) (m, 1 H, allyl CH), 6.21 (d, major, $^3J_{H,H} = 6.2$) and 6.42 (br, minor) (1 H, C^2H of coord. Ph), 7.23 (t, $^3J_{H,H} = 7.8$, 0.5 H, C^4H of coord. Ph, major), 7.32−7.58 (13.5 H); 7.66−7.73 (m, 2.5 H); 7.85 (m, 0.5 H, C^5H of coord. Ph, major), 8.03−8.23 (m, 4 H, arom). ^{31}P NMR (202.5 MHz, CD_2Cl_2, −90 °C): δ 148.8 (s, 54%), 148.1 (s, 46%).

X-Ray Structure of (S_a,R_C,R_C,S_{Pd})-3a. A green crystal of (S_a,R_C,R_C,S_{Pd})-**3a** (formed *in situ*) was obtained by layering hexane over a CH_2Cl_2 solution of the diasteromeric mixture of **3** (containing the racemic ligand (S_a,R_C,R_C+R_a,S_C,S_C)-**1**) in an NMR tube. Crystal data: $C_{39}H_{35}NO_2PPdSb$, orthorhombic, $P2_12_12_1$, 0.49 × 0.38 × 0.20 mm, $a = 11.1708(3)$ Å, $b = 14.5431(4)$ Å, $c = 21.6740(6)$ Å, $V = 3521.12(17)$ Å^3, $Z = 4$, $F(000) = 1\,832$, $D_{calcd} = 1.741$ g cm^{-3}, $\mu = 1.392$ mm^{-1}. Data were collected at 200 K on a Bruker AXS SMART APEX platform in the θ range 1.69−28.30°. The structure was solved with SHELXTL using direct methods. Of the 65 196 measured ($-14 \le h \le 14$, $-19 \le k \le 19$, $-28 \le l \le 28$), 8751 unique reflections were used in the refinement (full-matrix least-squares on F^2 with anisotropic displacement parameters). $R_1 = 0.0207$ (8571 data with $F_o > 4\sigma(F_o)$), $wR_2 = 0.0546$ (all data). Max. and min. difference peaks were +0.858 and −0.370 e Å^{-3}.

[RhCl(NBD)(1)] (4a). $[Rh(NBD)Cl]_2$ (0.0922 g, 0.0002 mol) and ligand **1** (0.2158 g, 0.0004 mol) were dissolved in CH_2Cl_2 (10 mL), and the resulting solution was stirred for 1 h at room temperature. The solvent was evaporated, and the resulting yellow powder was washed with a small amount of diethyl ether and pentane and dried in air and then under vacuum (0.05 mm). Yield: 0.2897 g, 94%. $[\alpha]_D^{20} = +196$ (c 0.25). Anal. Calcd for $C_{43}H_{38}NO_2PClRh$: C, 67.06; H, 4.97; N, 1.82. Found: C, 67.13; H, 5.12; N, 1.77. HRMS (MALDI): calcd for $C_{43}H_{38}NO_2PRh$ 734.1690, found 734.1697 $[M - Cl]^+$. ^{13}C NMR (75.47 MHz, $CDCl_3$): δ 20.4 (d, $^3J_{P,C} = 4.7$, NCHCH_3), 50.3 (d, $^1J_{Rh,C} = 10.8$), 55.0 (d, $^1J_{Rh,C} = 10.7$, CH=CH *trans* to Cl), 50.6, 50.7 (CHCH=CH), 55.2 (d, $^2J_{P,C} = 13.1$, N$CHCH_3$), 64.1 (d, $J_{P,C} = 4.7$, NBD CH_2), 93.4 (dd, $^1J_{Rh,C} = 3.3$,$^2J_{P,C} = 15.5$), 91.5 (dd, $^1J_{Rh,C} = 2.9$,$^2J_{P,C} = 16.3$, CH=CH *trans* to P), 120.7, 121.4 (d, $J_{P,C} = 2.1$), 123.5 (d, $J_{P,C} = 3.8$), 125.0, 125.1 (d, $J_{P,C} = 2.9$), 125.04, 125.4, 126.2, 126.3, 126.8, 126.9, 127.2, 127.8, 128.0, 128.1, 128.6, 129.9, 130.0, 130.8 (d, $J_{P,C} = 0.9$), 131.8 (d, $J_{P,C} = 1.5$), 132.3 (d, $J_{P,S} = 2.1$), 132.5 (d, $J_{P,C} = 1.4$), 144.0 (d, $J_{P,C} = 3.0$), 148.9 (d, $J_{P,C} = 4.0$), 149.6 (d, $^3J_{P,C} = 1.4$), 149.8 (d, $^3J_{P,C} = 1.4$) (arom.). ^1H NMR (300.13 MHz,

(50) Mikhel, I. S.; Bernardinelli, G.; Alexakis, A. *Inorg. Chim. Acta* **2006**, *359*, 1826.

$CDCl_3$): δ 1.22 (br s, 2 H, NBD CH_2), 1.34 (d, $^3J_{H,H}$ = 7.2, 6 H, NCHCH_3), 2.61 (br m, 1 H, NBD CH=CH), 3.04 (br m, 1 H, NBD CH=CH), 3.63 (br m, 2 H, NBD CH), 5.31 (br m, 1 H, NBD CH=CH), 5.32 (dq ($^3J_{H,H}$ = 7.1, $^3J_{P,H}$ = 10.6, 2 H, NCHCH$_3$), 5.50 (br m, 1 H, NBD CH=CH), 7.14 (d, $^3J_{H,H}$ = 8.8, 1 H), 7.18−7.44 (m, 11 H), 7.49−7.57 (m, 5 H), 7.73 (d, $^3J_{H,H}$ = 8.8, 1 H), 7.83 (d, $^3J_{H,H}$ = 8.1, 1 H), 8.09 (d, $^3J_{H,H}$ = 8.2, 1 H), 8.25 (d, $^3J_{H,H}$ = 8.8, 1 H), 8.42 (d, $^3J_{H,H}$ = 8.8, 1 H) (arom.). ^{31}P NMR (121.49 MHz, $CDCl_3$): δ 136.7 (d, $^1J_{Rh,P}$ = 280 Hz).

X-Ray Structure Determination of (S_a,R_C,R_C)-4a. Yellow crystals of **4a** were obtained by slow evaporation of a CH_2Cl_2/Et_2O/C_6H_{14} solution. Crystal data: $C_{43}H_{38}ClNO_2PRh$, orthorhombic, $P2_12_12_1$, 0.42 × 0.35 × 0.17 mm, a = 9.0520(5) Å, b = 11.3595(6) Å, c = 34.266(2) Å, V = 3523.5(3) Å^3, Z = 4, F(000) = 1584, D_{calcd} = 1.4524 g cm^{-3}, μ = 0.645 mm^{-1}. Data were collected at 200 K on a Bruker AXS SMART APEX platform in the θ range 1.89−26.37°. The structure was solved with SHELXTL using direct methods. Of the 32 027 measured ($-11 \le h \le 11$, $-14 \le k \le 14$, $-42 \le l \le 42$), 7222 unique reflections were used in the refinement (full-matrix least-squares on F^2 with anisotropic displacement parameters). R_1 = 0.0285 (6951 data with $F_o > 4\sigma(F_o)$), wR_2 = 0.0687 (all data). Max. and min. difference peaks were +0.589 and −0.202 e Å^{-3}.

[RhCl(COD)(1-κP)] (4b). [RhCl(COD)]$_2$ (0.0986 g, 0.0002 mol) and ligand **1** (0.2158 g, 0.0004 mol) were dissolved in CH_2Cl_2 (10 mL), and the resulting solution was stirred for 1 h at room temperature. After evaporating the solvent, the residue was purified by flash chromatography under argon pressure: R_f 0.55 (2:1 (v/v) pentane/Et_2O). The solvent was evaporated, and the resulting yellow powder was dried under vacuum (0.05 mm). Yield: 0.2810 g, 89%. $[\alpha]_D^{20}$ = +181 (c 0.25). Anal. Calcd for $C_{44}H_{42}NO_2PClRh$: C, 67.22; H, 5.38; N, 1.78. Found: C, 67.47; H, 5.20; N, 1.77. HRMS (MALDI): calcd for $C_{44}H_{42}NO_2PRh$ 750.2003, found 750.2005 [M − Cl]$^+$. ^{13}C NMR (75.47 MHz, $CDCl_3$): δ 19.9 (d, $^3J_{P,C}$ = 4.4, NCHCH$_3$), 28.09 (d, $J_{P,C}$ = 1.4), 28.14 (d, $J_{P,C}$ = 2.0), 31.9 (d, $J_{P,C}$ = 1.5), 33.5 (d, $J_{P,C}$ = 2.4, CH$_2$CH=CH); 55.5 ($^2J_{P,C}$ 13.1, NCHCH$_3$), 69.2 (d, $^1J_{Rh,C}$ = 12.8), 74.0 (d, $^1J_{C,Rh}$ =13.6, CH$_2C$H=CH *trans* to Cl), 110.4 (dd, $^1J_{Rh,C}$ = 5.9,$^2J_{P,C}$ = 15.5), 111.4 (dd, $^1J_{Rh,C}$ 5.7,$^2J_{P,C}$ = 16.3, CH$_2C$H=CH *trans* to P), 120.6, 120.9 (d, $J_{P,C}$ = 2.1), 123.6 (d, $J_{P,C}$ = 4.0), 125.0, 125.04, 125.08, 125.5, 126.3 (d, $J_{P,C}$ = 4.4), 126.87, 126.93, 127.2, 127.9, 128.0, 128.2, 128.5, 130.0 (d, $J_{P,C}$ = 1.2), 130.1, 130.8 (d, $J_{P,C}$ = 0.8), 131.8 (d, $J_{P,C}$ = 1.7), 132.4 (d, $J_{P,C}$ = 2.3), 132.6 (d, $J_{P,C}$ = 1.1), 144.2 (d, $J_{P,C}$ = 2.7), 148.8 (d, $J_{P,C}$ = 3.8), 149.9 (d, $^3J_{P,C}$ = 1.1), 150.1 ($^3J_{P,C}$ = 1.1) (arom.). ^{1}H NMR (300.13 MHz, $CDCl_3$): δ 1.16 (m, 1 H, COD CHH′), 1.40 (d, $^3J_{H,H}$ = 7.1, 6H, NCHCH_3), 1.44 (m, 1 H, COD CHH′), 1.86−2.25 (m, 5 H, COD CHH′), 2.37 (m, 1 H, CHH′), 2.89 (br m, 1 H, COD CH=CH), 4.03 (br m, 1 H, COD CH=CH), 5.48 (dq, $^3J_{H,H}$ = 7.0, $^3J_{P,H}$ = 11.9, 2H, NCHCH$_3$), 5.58 (br m, 1 H, COD CH=CH), 5.69 (br m, 1 H, COD CH=CH), 7.06 (d, $^3J_{H,H}$ = 8.9, 1 H), 7.14−7.42 (m, 11 H), 7.47−7.55 (m, 5 H), 7.65 (d, $^3J_{H,H}$ = 8.8, 1 H), 7.81 (d, $^3J_{H,H}$ = 8.1, 1 H), 8.04 (d, $^3J_{H,H}$ = 8.2, 1 H), 8.19 (d, $^3J_{H,H}$ = 8.8, 1 H), 8.46 (d, $^3J_{H,H}$ = 8.8, 1 H) (arom.). ^{31}P NMR (121.49 MHz, $CDCl_3$): δ 133.6 (d, $^1J_{Rh,P}$ = 246.8).

X-Ray Structure Determination of (S_a,R_C,R_C)-4b. Yellow crystals of **4b** were obtained by slow evaporation of an Et_2O solution. Crystal data: $C_{44}H_{42}ClNO_2PRh$, orthorhombic, $P2_12_12_1$, 0.79 × 0.49 × 0.21 mm, a = 12.0520(12) Å, b = 12.7854(13) Å, c = 23.726(2) Å, V = 3655.9(6) Å^3, Z = 4, F(000) = 1624, D_{calcd} = 1.428 g cm^{-3}, μ = 0.623 mm^{-1}. Data were collected at 200 K on a Bruker AXS SMART APEX platform in the θ range 1.90−27.49°. The structure was solved with SHELXTL using direct methods. Of the 35 600 measured ($-15 \le h \le 15$, $-16 \le k \le 16$, $-30 \le l \le 30$), 8382 unique reflections were used in the refinement (full-matrix least-squares on F^2 with anisotropic displacement parameters). R_1 = 0.0342 (7897 data with $F_o > 4\sigma(F_o)$), wR_2 = 0.0794 (all data). Max. and min. difference peaks were +0.793 and −0.339 e Å^{-3}.

[Rh(NBD)(1,2-η-Ph-1-κP)]SbF$_6$ (5a). [Rh(NBD)Cl]$_2$ (0.0461 g, 0.0001 mol) and ligand **1** (0.1079 g, 0.0002 mol) were dissolved in CH_2Cl_2 (10 mL), and the resulting solution was stirred for 1 h at room temperature and then was added to $AgSbF_6$ (0.0687 g, 0.0002 mol). The resulting slurry was stirred for 2 h, after which AgCl was filtered off. The filtrate was rinsed with CH_2Cl_2 (4 mL). The clear solution was evaporated to dryness, and the resulting yellow-orange powder was washed with a small amount of diethyl ether (twice) and pentane and dried in air and then under vacuum (0.05 mm). Yield: 0.1786 g, 92%. $[\alpha]_D^{20}$ = +156 (c 0.25). Anal. Calcd for $C_{43}H_{38}NO_2F_6PRhSb$: C, 53.22; H, 3.95; N, 1.44. Found: C, 53.51; H, 4.20; N, 1.49. HRMS (MALDI): calcd for $C_{43}H_{38}NO_2PRh$ 734.1690, found 734.1682 [M − SbF$_6$]$^+$. ^{13}C NMR (125.78 MHz, CD_2Cl_2, −80 °C): δ 19.7 (free NCHCH), 23.6 (coord. NCHCH$_3$), 49.0, 49.3 (NBD CHCH=CH), 51.8 (d, $^2J_{P,C}$ = 21.6, coord. NCHCH$_3$), 53.4 (d, $^2J_{P,C}$ = 7.0, free NCHCH$_3$), 57.9 (d, $^1J_{Rh,C}$ = 8.6), 63.3 (d, $^1J_{Rh,C}$ = 7.9, CH$_2C$H=CH *trans* to Cl), 70.9 (NBD CH_2), 99.9 (d, $^2J_{P,C}$ = 13.9), 102.1 (d, $^2J_{P,C}$ = 14.6, CH$_2C$H=CH *trans* to P), 103.7 (C^2 of coord. Ph), 120.8, 121.7, 122.1, 126.3, 126.0, 126.2, 126.9, 127.0, 127.1, 128.0 (C^6 of coord. Ph), 128.1 (C^2 and C$_6$ of free Ph), 128.2 (C^4 of free Ph), 128.3 (C^4 of coord. Ph), 128.7 (C^1 of coord. Ph), 128.8 (C^3 and C^5 of free Ph), 129.0, 131.4 (C^5 of coord. Ph), 131.5, 131.69, 131.73, 132.0, 132.1, 135.5 (C^3 of coord. Ph), 138.9 (C^1 of free Ph), 147.0, 147.1, 147.4 (d, $^3J_{P,C}$ = 5.5) (arom.). ^{1}H NMR (500.23 MHz, CD_2Cl_2, −90 °C): δ 1.40 (br, 3 H, free NCHCH_3), 1.45 (d, $^3J_{H,H}$ = 8.4) and 1.59 (d, $^3J_{H,H}$ 8.2, 2 H, NBD CH_2), 2.15 (br, 3 H, coord. NCHCH_3), 3.09 (br s, 1 H, NBD CH=CH *trans* to Cl), 3.39 and 3.50 (br s, 2H, NBD CH), 3.65 (br s, 1 H, NBD CH=CH *trans* to P), 4.07 (dq $^3J_{P,H}$ = 41.3, $^3J_{H,H}$ = 6.1, 1H, coord. NCHCH$_3$), 4.08 (br s, 1 H, NBD CH=CH *trans* to P), 4.28 (br m, 1 H, NBD CH=CH *trans* to Cl), 4.51 (m, $^3J_{P,H}$ = 6.4, $^3J_{H,H}$ = 6.4, 1 H, free NCHCH$_3$), 6.47 (br d, $^3J_{H,H}$ = 6.7, 1 H, coord. C$_2H$), 7.20−7.44 (m, 10 H), 7.49−7.67 (m, 6 H), 8.04 (d, $^3J_{H,H}$ = 8.2, 1 H), 8.10 (d, $^3J_{H,H}$ = 8.7, 1 H), 8.11 (d, $^3J_{H,H}$ = 7.3, 1 H) 8.17 (d, $^3J_{H,H}$ = 8.9, 1 H), 8.32 (d, $^3J_{H,H}$ = 9.0, 1 H) (arom.). ^{31}P NMR (202.5 MHz, CD_2Cl_2): δ 138.9 (d, $^1J_{Rh,P}$ = 259.4).

X-Ray Structure Determination of (S_a,R_C,R_C+R_a,S_C,S_C)-5a. Slow evaporation of a MeOH solution of (*rac*)-**5a**, prepared by mixing (S_a,R_C,R_C)-**1** and (R_a,S_C,S_C)-**1** in 1:1 ratio, afforded orange platelets. Crystal data: $C_{43}H_{38}F_6NO_2PRhSb$, orthorhombic, $P2_12_12_1$, 0.28 × 0.22 × 0.07 mm, a = 11.2449(6) Å, b = 15.0329(8) Å, c = 22.3759(12) Å, V = 3 782.5(3) Å^3, Z = 4, F(000) = 1 936, D_{calcd} = 1.704 g cm^{-3}, μ = 1.262 mm^{-1}. Data were collected at 200 K on a Bruker AXS SMART APEX platform in the θ range 1.63−28.31°. The structure was solved with SHELXTL using direct methods. Of the 39 490 measured ($-14 \le h \le 14$, $-20 \le k \le 20$, $-29 \le l \le 29$), 9357 unique reflections were used in the refinement (full-matrix least-squares on F^2 with anisotropic displacement parameters). R_1 = 0.0374 (8 686 data with $F_o > 4\sigma(F_o)$), wR_2 = 0.0832 (all data). Max. and min. difference peaks were +0.987 and −0.338 e Å^{-3}. The value of the Flack parameter (−0.014(16)) indicated that the ligand in the crystal chosen had the (S_a,R_C,R_C) configuration.

[Rh(COD)(1,2-η-Ph-1-κP)]SbF$_6$ (5b). [RhCl(COD)]$_2$ (0.0493 g, 0.0001 mol) and ligand **1** (0.1079 g, 0.0002 mol) were dissolved in CH_2Cl_2 (10 mL). The resulting solution was stirred for 1 h at room temperature and then added to $AgSbF_6$ (0.0687 g, 0.0002 mol). The resulting slurry was stirred for 2 h, after which AgCl was filtered off. The filtrate was rinsed with CH_2Cl_2 (4 mL), and the clear solution was evaporated. The resulting yellow-orange powder was washed with a small amount of diethyl ether (twice) and pentane and dried in air and then under vacuum (0.05 mm). Yield: 0.1774 g, 90%. $[\alpha]_D^{20}$ = +201 (c 0.25). Anal. Calcd for $C_{44}H_{42}NO_2F_6PRhSb$: C, 53.57; H, 4.29; N, 1.42. Found: C, 53.86;

H, 4.41; N, 1.49. HRMS (MALDI): calcd for $C_{44}H_{42}NO_2PRh$ 750.2003, found 750.2000 $[M - SbF_6]^+$. ^{13}C NMR (125.78 MHz, CD_2Cl_2, −90 °C): δ 19.5 (free NCH*C*H_3), 24.8 (d, $J_{P,C} = 4.3$, coord. NCH*C*H_3), 24.3, 29.1, 30.5, 34.7 (*C*H_2CH═CH), 52.7 (d, $^2J_{P,C} = 20.4$, coord. N*C*HCH$_3$), 53.6 (d, $^2J_{P,C} = 7.0$, free N*C*HCH$_3$), 75.4 (d, $^1J_{Rh,C} = 11.3$), 82.9 (d, $^1J_{Rh,C} = 11.0$, CH_2*C*H═CH *trans* to Ph), 100.1 (C^2 of coord. Ph), 115.0 (d, $^2J_{P,C} = 12.2$), 119.0 ($^2J_{P,C} = 10.8$, CH_2*C*H═CH *trans* to P), 120.6, 121.4, 121.8, 122.5, 126.0, 126.3, 126.9, 127.0, 127.1, 127.2, 128.0 (C^2 and C^6 of free Ph), 128.18 (C^4 of free Ph), 128.23 (C^4 of coord. Ph), 128.6 (C^3 and C^5 of free Ph), 128.8, 129.0, 130.2 (C^6 of coord. Ph), 131.4, 131.5, 131.6, 131.8, 132.0, 132.2, 134.2 (C^5 of coord. Ph), 138.4 (C_1 of free Ph), 139.3 (C^1 of coord. Ph), 139.7 (C_3 of coord. Ph), 147.3, 147.39, 147.43 (arom). ^1H NMR (500.23 MHz, CD_2Cl_2, −90 °C): δ 1.16 (m, 1 H, COD C*H*$_2$), 1.42 (m, 1 H, COD C*H*$_2$), 1.53 (br, 3 H, free NCHC*H*$_3$), 1.68 (m, 2 H, COD C*H*$_2$), 1.89 (m, 1 H, COD C*H*$_2$), 2.08−2.25 (m, 2 H, COD C*H*$_2$ + 1 H, COD CH═CH *trans* to P), 2.25 (br, 3 H, coord. NCHC*H*$_3$), 2.44 (m, 1 H, COD C*H*$_2$), 2.59 (br m, 1 H, COD CH═CH *trans* to Ph), 4.08 (br d, $^3J_{P,H} = 45.1$, 1 H, coord. NC*H*CH$_3$), 4.58 (m, 1 H, free NC*H*CH$_3$), 4.59 (br m, 1 H, COD CH═CH *trans* to Ph), 5.22 (br m, 1 H, COD CH═CH *trans* to P), 6.56 (br s, 1 H, coord. C^2*H*), 7.16 (t, $^3J_{H,H} = 7.15$, 1 H, free C^4*H*), 7.23−7.69 (m, 14 H), 7.90 (br s, 1 H, coord. C^3H), 8.05 (d, $^3J_{H,H} = 8.1$, 1 H), 8.11 (d, $^3J_{H,H} = 8.1$, 1 H), 8.17 (d, $^3J_{H,H} = 8.8$, 1 H), 8.27 (d, $^3J_{H,H} = 8.8$, 1 H), 8.35 (d, $^3J_{H,H} = 8.8$, 1 H) (arom). ^{31}P NMR (202.5 MHz, CD_2Cl_2, −80 °C): δ 140.4 (d, $^1J_{Rh,P} = 224$).

(S_a,S_a,R_C,R_C,R_C,R_C)-[Rh(1-κP)(η⁶-Ph-1-κP)]SbF₆ (6). The racemic complex **5b**, prepared by mixing (S_a,R_C,R_C)-**1** and (R_a,S_C,S_C)-**1** in 1:1 ratio, (0.1042 g, 0.000106 mol) was dissolved in a small volume of MeOH (ca. 3 mL) and stored 1 week for crystallization. The solvent was carefully decanted, and the yellow-orange crystals were washed with MeOH (ca. 0.5 mL) and pentane (5 mL) and dried in air and then under vacuum (0.05 mm). Yield: 0.0441 g, 59%. Anal. Calcd for $C_{72}H_{60}N_2O_4F_6P_2RhSb$: C, 60.99; H, 4.27; N, 1.98. Found: C, 61.01; H, 4.45; N, 1.96. HRMS (MALDI): calcd for $C_{72}H_{60}N_2O_4P_2Rh$ 1181.3083, found 1181.3099 $[M - SbF_6]^+$. ^{13}C NMR (176.05 MHz, CD_2Cl_2, −90 °C): δ 18.6 (NCH*C*H$_3$ of free Ph, L1), 20.3 (NCH*C*H$_3$ of free Ph, L2), 20.8 (NCH*C*H$_3$ of free Ph, L2), 21.3 (NCH*C*H$_3$ of coord. Ph, L1), 48.4 (d, $^2J_{P,C} = 17.8$, N*C*HCH$_3$ of coord. Ph, L1), 52.6 (N*C*HCH$_3$ of free Ph, L2), 55.5 (N*C*HCH$_3$ of free Ph, L1), 56.7 (d, $^2J_{P,C} = 32.0$, N*C*HCH$_3$ of free Ph, L2), 98.4 (d, $^2J_{P,C} = 5.9$, C^4 of $Ph_{coord.}$), 102.9 (C^2 of coord. Ph), 103.0 (C^5 of coord. Ph), 109.0 (C^6 of coord. Ph), 112.4 (d, $^2J_{P,C} = 11.3$, C^1 of coord. Ph), 114.2 (C^3 of coord. Ph), 119.4, 120.1, 120.2, 120.5, 121.7, 123.1, 123.6, 124.7, 125.2, 125.6, 125.8, 125.9, 126.0, 126.2, 126.3, 126.4, 126.6, 126.7, 126.9, 127.7, 127.8, 128.2, 128.3, 128.5, 128.7, 129.0, 129.2, 129.7, 129.8, 130.0, 130.3, 130.5, 131.1, 131.3, 131.7, 131.9, 132.5, 132.7, 140.2, 143.7, 144.6, 146.8 (d, $J_{P,C} = 14.2$), 147.4, 147.8 (d, $^3J_{P,C} = 14.8$), 148.2 (d, $^3J_{P,C} = 6.2$) (arom). ^1H NMR (700.13 MHz, CD_2Cl_2, −90 °C); δ 0.51 (br s, 3 H, NCHC*H*$_3$ of free Ph, L2), 0.62 (br s, 3 H, NCHC*H*$_3$ of free Ph, L1), 1.04 (br s, 3 H, NCHC*H*$_3$ of free Ph, L2), 1.75 (br s, 3 H, NCHC*H*$_3$ of coord. Ph, L1), 3.81 (br d, $^3J_{P,H} = 39.4$, 1 H, NC*H*CH$_3$ of coord. Ph, L1), 4.34 (m, 1 H, NC*H*CH$_3$ of free Ph, L2), 4.37 (m, 1 H, NC*H*CH$_3$ of free Ph, L1), 4.98 (m, 1 H, C_2*H* of coord. Ph), 5.78 (m, 2 H, NC*H*CH$_3$ of free Ph, L2 + naphth.), 6.10 (d, $^3J_{H,H} = 7.9$, 1 H), 6.22 (m, 1 H, C_4*H* of coord. Ph), 6.32 (d, $^3J_{H,H} = 7.1$, 1 H), 6.37 (d, $^3J_{H,H} = 7.4$, 1 H) 6.55 (m, 1 H), 6.70 (m, 1 H), 6.77 (d, $^3J_{H,H} = 8.5$, 1 H), 6.82 (m, 1 H), 6.87 (m, 1 H), 6.97 (d, $^3J_{H,H} = 8.1$, 1 H), 7.02 (m, 1 H), 7.11−7.35 (m, 16 H), 7.42 (d, $^3J_{H,H} = 8.1$, 1 H), 7.49 (d, $^3J_{H,H} = 7.1$, 1 H) 7.67 (s, 1 H), 7.75 (d, $^3J_{H,H} = 7.4$, 1 H), 7.80−7.87 (m, 5 H), 8.03 (m, 2 H), 8.08 (d, $^3J_{H,H} = 7.1$, 1 H), 8.17 (d, $^3J_{H,H} = 7.5$, 1 H), 8.43 (d, $^3J_{H,H} = 7.8$, 1 H), 8.56 (d, $^3J_{H,H} = 7.3$, 1 H) (arom). ^{31}P NMR (283.42 MHz, CD_2Cl_2, −90 °C): δ 150.5 (dd, $^1J_{Rh,P} = 314$, $^2J_{P,P}$ 21.4, L1), 147.3 (dd, $^1J_{Rh,P} = 327$, $^2J_{P,P} = 21.4$, L2).

X-Ray of (S_a,S_a,R_C,R_C,R_C,R_C)-[Rh(1-κP)(η⁶-Ph-1-κP)]SbF₆ (6). Orange crystals of **6** were obtained with racemic **5b**, prepared by mixing (S_a,R_C,R_C)-**1** and (R_a,S_C,S_C)-**1** in 1:1 ratio, by slow evaporation from MeOH. Crystal data: $C_{150}H_{139}F_{12}N_4O_{14}P_4Rh_2Sb_2$, monoclinic, $P2_1/n$, 0.31 × 0.28 × 0.20 mm, $a = 25.143(5)$ Å, $b = 21.055(4)$ Å, $c = 26.124(5)$ Å, $V = 13\,829(5)$ Å^3, $Z = 4$, $F(000) = 6\,156$, $D_{calcd} = 1.452$ g cm^{-3}, $\mu = 0.747$ mm^{-1}. Data were collected at 200 K on a Bruker AXS SMART APEX platform in the θ range 1.12−21.98°. The structure was solved with SHELXTL using direct methods. Of the 73 480 measured ($-26 \le h \le 26$, $-22 \le k \le 22$, $-27 \le l \le 27$), 16 925 unique reflections were used in the refinement (full-matrix least-squares on F^2 with anisotropic displacement parameters). $R_1 = 0.0657$ (8351 data with $F_o > 4\sigma(F_o)$), $wR_2 = 0.1753$ (all data). Max. and min. difference peaks were +0.668 and −1.031 e Å^{-3}.

X-ray of (S_a,R_C,R_C+R_a,S_C,S_C)-[RuCl₂(η⁶-Ph-1,κP)] (7). Starting from the racemic ligand, obtained by mixing (S_a,R_C,R_C)-**1** and (R_a,S_C,S_C)-**1** in 1:1 ratio, **7** was prepared according to the published procedure.[10a] Red platelets were obtained by crystallization from CH_2Cl_2/hexane. Crystal data: $C_{36}H_{30}Cl_2NO_2PRu$, monoclinic, $P2_1/c$, 0.46 × 0.14 × 0.04 mm, $a = 17.8778(11)$ Å, $b = 9.1563(6)$ Å, $c = 18.4977(11)$ Å, $V = 3\,034.4(3)$ Å^3, $Z = 4$, $F(000) = 1\,448$, $D_{calcd} = 1.558$ g cm^{-3}, $\mu = 0.781$ mm^{-1}. Data were collected at 200 K on a Bruker AXS SMART APEX platform in the θ range 2.26−27.10°. The structure was solved with SHELXTL using direct methods. Of the 28 232 measured ($-22 \le h \le 22$, $-12 \le k \le 12$, $-23 \le l \le 23$), 6695 unique reflections were used in the refinement (full-matrix least-squares on F^2 with anisotropic displacement parameters). $R_1 = 0.0321$ (5932 data with $F_o > 4\sigma(F_o)$), $wR_2 = 0.0806$ (all data). Max. and min. difference peaks were +0.786 and −0.326 e Å^{-3}.

Acknowledgment. A.M. thanks Professor Paul S. Pregosin for helpful discussions.

Supporting Information Available: CIF files of **3**, **4a**, **4b**, **5a**, **6**, and **7**. This material is available free of charge at http://pubs.acs.org.

OM800064R